

SIMULATED FMRI TOOLBOX

A THESIS SUBMITTED TO  
THE GRADUATE SCHOOL OF INFORMATICS  
OF  
THE MIDDLE EAST TECHNICAL UNIVERSITY

BY

KEMAL DOĐUŐ TÜRKEY

IN PARTIAL FULFILLMENT OF THE REQUIREMENTS FOR THE DEGREE OF  
MASTER OF SCIENCE  
IN  
THE DEPARTMENT OF MEDICAL INFORMATICS

DECEMBER 2009

Approval of the Graduate School of Informatics

\_\_\_\_\_  
Prof. Dr. Nazife BAYKAL  
Director

I certify that this thesis satisfies all the requirements as a thesis for the degree of Master of Science.

\_\_\_\_\_  
Prof. Dr. Nazife BAYKAL  
Head of Department

This is to certify that we have read this thesis and in that in our opinion it is fully adequate, in scope and quality, as a thesis for the degree of Master of Science.

\_\_\_\_\_  
Assist. Prof. Dr. Didem GÖKÇAY  
Supervisor

Examining Committee Members

Assist. Prof. Dr. Alptekin TEMİZEL	(METU, II)	_____
Assist. Prof. Dr. Didem GÖKÇAY	(METU, II)	_____
Assoc. Prof. Dr. Kemal ARDA	(Onkoloji Has.)	_____
Prof. Dr. Bülent CELASUN	(Gören Patoloji)	_____
Assist. Prof. Dr. Erhan EREN	(METU, II)	_____

**I hereby declare that all information in this document has been obtained and presented in accordance with academic rules and ethical conduct. I also declare that, as required by these rules and conduct, I have fully cited and referenced all material and results that are not original to this work.**

**Name, Last name : Kemal Dođuř TÜRKEY**

**Signature : \_\_\_\_\_**

# **ABSTRACT**

## **SIMULATED FMRI TOOLBOX**

TÜRKAY, Kemal Dođuş

M.S., Department of Medical Informatics

Supervisor: Assoc. Prof. Dr. Didem GÖKÇAY

December 2009, 71 pages

In this thesis a simulated fMRI toolbox is developed in order to generate simulated data to compare and benchmark different functional magnetic resonance image analysis methods. This toolbox is capable of loading a high resolution anatomic brain volume, generating 4D fMRI data in the same data space with the anatomic image, and allowing the user to create block and event-related design paradigms. Common fMRI artifacts such as scanner drift, cardiac pulsation, habituation and task related or spontaneous head movement can be incorporated into the 4D fMRI data. Input to the toolbox is possible through MINC 2.0 file format, and output is provided in ANALYZE format. The major contribution of this toolbox is its

facilitation of comparison of fMRI analysis methods by generating several different fMRI data under varying noise and experiment parameters.

Keywords: Functional magnetic resonance imaging, fMRI, simulation, fMRI data generation.

# ÖZ

## FMRI SIMÜLASYONU UYGULAMASI

TÜRKAY, Kemal Doęuş

Yüksek Lisans, Tıp Bilişimi

Tez Yöneticisi: Doç. Dr. Didem GÖKÇAY

Aralık 2009, 71 sayfa

Bu tez çalışmasında, farklı fonksiyonel manyetik rezonans görüntüleme analizi metodlarını karşılaştırmak ve değerlendirmek amacıyla simule edilmiş veri yaratmak için bir simule edilmiş fMRG uygulaması geliştirilmiştir. Bu uygulama, yüksek çözünürlüklü anatomik beyin görüntülerini yükleyebilme, anatomik beyin görüntüsü ile aynı veri alanında 4 boyutlu fMRG verisi yaratabilme ve kullanıcıya blok ve uyarana bağlı deney tasarımı yaptırabilme yeteneklerine sahiptir. Tarayıcı kayması, kalp atışları, alışma ve kafa hareketleri gibi sık görülen fMR görüntüleme parazitleri 4D fMRI verisi ile birleştirildi. Uygulamaya girdi MINC 2.0 dosya formatı ile mümkündür, çıktı ise ANALYZE formatı ile sağlanır. Bu uygulamanın en büyük katkısı, fMRI analiz

metodlarının deęişen gürültü ve deney parametreleri altında birbirinden farklı fMRG verisi yaratarak fMRG analiz metodlarının karşılaştırılmasını kolaylaştırmasıdır.

Anahtar Kelimeler: Fonksiyonel manyetik rezonans görüntüleme, fMRG, simülasyonu, fMRG verisi üretme.

To my beloved one for her everlasting support



## **ACKNOWLEDGEMENTS**

I would like to give special thanks to my thesis supervisor, Assoc. Prof. Dr. Didem GÖKÇAY for her professional support, guidance and encouragements which were invaluable for me during this thesis' preparation.

## TABLE OF CONTENTS

ABSTRACT.....	iv
ÖZ.....	vi
ACKNOWLEDGEMENTS.....	ix
TABLE OF CONTENTS.....	x
LIST OF TABLES.....	xii
LIST OF FIGURES.....	xiii
CHAPTER	
1. INTRODUCTION.....	1
2. BACKGROUND AND LITERATURE SURVEY .....	4
2.1 MRI simulators.....	4
2.2 Functional Magnetic Resonance Imaging Process.....	5
2.3 fMRI design paradigms.....	7
2.3.1 Block design paradigm.....	7
2.3.2 Event-related design paradigm .....	8
2.4 fMRI artifacts .....	9
2.4.1 Scanner drift.....	9
2.4.2 Cardiac pulsation .....	10
2.4.3 Habituation.....	11
2.4.4 Subject Motion.....	11
2.5 FSL’s POSSUM .....	12
3. METHODS .....	14
3.1 Components Of The METU-fMRISim.....	14

3.1.1	Simulated anatomic brain volume .....	17
3.1.2	4D fMRI data generation.....	18
3.1.3	Block paradigm.....	20
3.1.4	Event-related paradigm .....	22
3.1.5	Artifacts .....	26
3.1.6	Optional gaussian convolution in spatial domain.....	32
3.1.7	Correlated head movement .....	33
3.1.8	Spontaneous head movement.....	36
3.1.9	Final fMRI data.....	38
4.	RESULTS .....	41
4.1	Artifact tests.....	43
4.2	Motion tests with AFNI .....	46
5.	CONCLUSION .....	52
	REFERENCES .....	54
	APPENDIX	
A.	Anatomical Directions and Planes .....	57

## LIST OF TABLES

<b>Table 1</b> The main components of the simulator.....	14
--	----

## LIST OF FIGURES

<b>Figure 1</b>	Overview of the MRI Simulator – SIMRI.....	5
<b>Figure 2</b>	Typical fMRI experiment.....	6
<b>Figure 3</b>	Intensity change over time in fMRI.....	7
<b>Figure 4</b>	Finger tapping experiment.....	8
<b>Figure 5</b>	Hemodynamic response from an activated voxel.....	9
<b>Figure 6</b>	POSSUM’s GUI ( <a href="http://www.fmrib.ox.ac.uk/fsl/possum/index.html">http://www.fmrib.ox.ac.uk/fsl/possum/index.html</a> )....	13
<b>Figure 7</b>	Components of the simulator.....	16
<b>Figure 8</b>	A study consists of $i$ volumes.....	19
<b>Figure 9</b>	GUI of the 4D fMRI data generation.....	19
<b>Figure 10</b>	(A) Initial signal $f(i)$ , (B) Block paradigm added signal $b(i)$ with the following parameters: Baseline Value=20; Volume Count=100; Lag=0.....	21
<b>Figure 11</b>	GUI of block paradigm.....	21
<b>Figure 12</b>	(Left) GUI of event-related paradigm, (Right) File format of the event points.....	23
<b>Figure 13</b>	Impulse response function.....	24
<b>Figure 14</b>	(A) Initial signal $f(i)$ , (B) Event-related paradigm added signal $e(i) * g_t(i)$ .....	25
<b>Figure 15</b>	Multiple hot-spot selection.....	26
<b>Figure 16</b>	(A) Block paradigm added signal $b(i) * g_m(i)$ , (B) After addition of scanner drift $b(i) * g_m(i) + d(i)$ , where $a$ is 0.4.....	27
<b>Figure 17</b>	GUI of scanner drift.....	27

<b>Figure 18</b> Pulse sequence between two TRs. ....	28
<b>Figure 19</b> (A) Block paradigm added signal $b(i) * g_m(i)$ , (B) After addition of cardiac pulsation $b(i) * g_m(i) + c(i)$ . ....	29
<b>Figure 20</b> GUI of cardiac pulsation.....	30
<b>Figure 21</b> Loss ratio (slope).....	31
<b>Figure 22</b> (A) Block paradigm added signal $b(i) * g_m(i)$ , (B) After addition of habituation $b(i) * g_m(i) + h(i)$ , where m is 0.1 .....	31
<b>Figure 23</b> GUI of gaussian convolution in spatial domain .....	33
<b>Figure 24</b> GUI of correlated head movement.....	35
<b>Figure 25</b> (Left) GUI of spontaneous head movement, (Right) File structure for spontaneous head movement.....	37
<b>Figure 26</b> The main GUI of the simulator. ....	39
<b>Figure 27</b> Real MR data.....	42
<b>Figure 28</b> Time series of selected voxel. ....	42
<b>Figure 29</b> The groundtruth data. (O).....	43
<b>Figure 30</b> First simulated data ( $S_a$ ). ....	44
<b>Figure 31</b> Second simulated data ( $S_b$ ).....	44
<b>Figure 32</b> Third simulated data ( $S_c$ ).....	44
<b>Figure 33</b> Fourth simulated data ( $S_d$ ). ....	45
<b>Figure 34</b> The motion components of the <b>first</b> data (without motion) where the first 3 rows indicate translation in mm and last 3 rows indicate rotation along 3 axes in degrees.....	48
<b>Figure 35</b> The motion components of the <b>second</b> data (without motion) .....	49
<b>Figure 36</b> The motion components of the <b>first</b> data (with motion).....	50
<b>Figure 37</b> The motion components of the <b>second</b> data (with motion).....	51

# CHAPTER 1

## INTRODUCTION

Magnetic Resonance Imaging (MRI) is a medical imaging technique most commonly used in radiology to visualize the internal structure of the body. MRI provides more valuable visual output for soft tissues of the body compared to other imaging tools such as computed tomography (CT), and this advantage makes it especially useful in neurological, musculoskeletal, cardiovascular and oncological imaging. MRI uses a powerful magnetic field to align the nuclear magnetization of hydrogen atoms of water in body, while CT imaging uses ionizing radiation. Radio frequency (RF) fields are used to systematically arrange the alignment of the magnetization, causing the hydrogen nuclei to produce a rotating magnetic field detectable by the scanner. This signal can be manipulated by additional magnetic fields to build up enough information to construct an image of the body.

Functional Magnetic Resonance Imaging (fMRI) is a specialized type of MRI scan. fMRI measures the hemodynamic response related to neural activity in the soft tissues like the brain or spinal cord of humans or other animals. The main mechanism that fMRI relies on, is the BOLD (Blood-oxygen-level dependent) which is based on the fact that active tissue consumes more oxygen than others. Using the intensities obtained in fMRI, brain activation maps can be derived by statistical inference. fMRI has dominated

brain mapping field due to the nature of the MRI that takes the advantages of low invasiveness, lack of radiation exposure, relatively wide availability and superior resolution in comparison to other neuroimaging methods.

Since MRI is relatively new technology (The first studies on humans were published in 1977), the literature and research in this area has been rapidly growing. The statistical nature of the activity prediction process in fMRI analysis produces brain activity maps that are prone to high variability with respect to the parameters of the activity detection method. New analysis methods of fMR images are proposed and published almost on a monthly basis. Sometimes these methods produce very different results but there is no gold standard to show us which method is more reliable than the others. The need for such a gold standard is the main motivation of this thesis.

In the context of this thesis, a software platform is produced in order to generate simulated data to compare and benchmark different fMRI analysis methods. There are some MRI simulators publicly available and widely used, but to the best of our knowledge, there is only one fMRI simulator and it is especially specialized mainly on the physics of the MRI and does not give the user extensive choices to add artifacts that are commonly seen in fMRI experiments, as well as options to construct an fMRI time series based on stimulus paradigms.

While developing this application, the main purpose was to produce practical and sharable software based on fMRI experimental paradigms and modulate the output of the fMRI signal due to not only physical, but also cognitive processes.

With the advantage of creating an fMRI signal from scratch (in desired temporal and also spatial dimensions) it is possible to compare fMRI analysis methods and find out the boundaries in which the analysis methods work effectively.

In fMRI studies it is impossible to acquire a pure signal; there are always some artifacts in the fMRI time series. A realistic fMRI simulator should contain certain types of



artifacts. By the manipulation of artifact conditions the performance of the fMRI analysis methods can be documented. In reality, once the fMRI data acquisition is complete, it is almost impossible to manipulate a specific artifact with new parameters. For example, while the slope of signal drift may be 15% in an fMRI study, the slope can be 30% in another study, but in presence of other artifacts, it is difficult to take apart drift alone, and manipulate exclusively. Therefore we developed a test bed for generating various different 4D fMRI data, given specific experimental paradigms.

The layout of this thesis as follows: In chapter 2, background and literature survey is represented, in chapter 3 methods which were used in order to implement this toolbox is discussed, followed by results and conclusion in chapter 4 and 5 .

## CHAPTER 2

### BACKGROUND AND LITERATURE SURVEY

#### 2.1 MRI simulators

MRI simulation is an important counterpart to MRI acquisitions. MRI simulation permits the investigation of artifact causes and effects. Likewise simulation may help in the development and optimization of MR sequences. Finally, with the increased interest in computer-aided MR image analysis methods (for example: segmentation, data fusion, quantization), an MRI simulator provides an interesting assessment tool since it generates 3D realistic images from medical virtual objects perfectly known. Currently, there are a variety of MRI simulators SIMRI (Benoit, 2004), McBIC's MRI Simulator (Cocosco, 1997), JEMRIS (Vahedipour, 2008) and ODIN (Jochimsen, 2004), however, the issues that are dealt with by these simulators are profoundly different than our approach to fMRI simulation.

MRI simulators use the electromagnetic Bloch equations in physics to model the change in magnetic field and generate intensities accordingly. A hypothetical simulator overview is given below in Figure 1. From a 3D virtual object, the static field definition and MRI sequence, the magnetization kernel computes a set of RF signals, i.e. the k-space. In order to simulate realistic images, noise can be added to the k-space, which can

be filtered like in a real imager before the reconstruction of the MR image using Fast Fourier transform (Benoit, 2004).

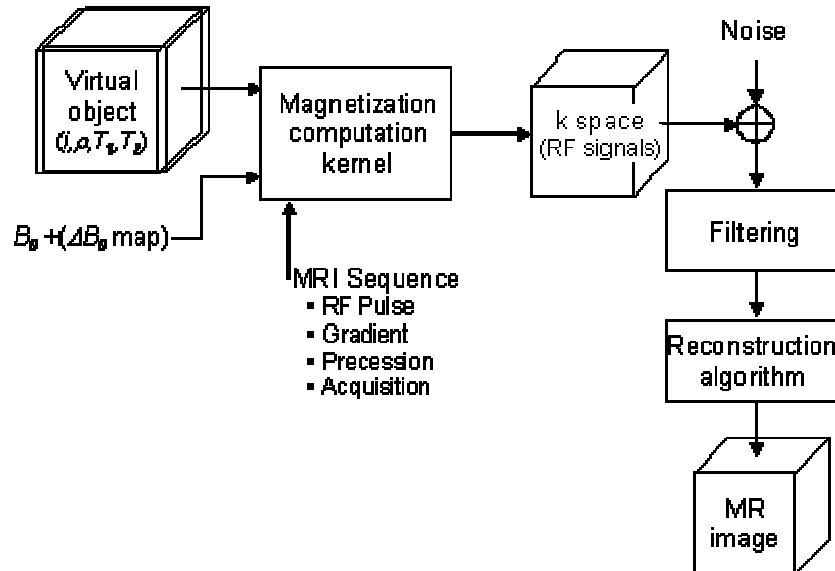


**Figure 1** Overview of the MRI Simulator – SIMRI (image taken from SIMRI’s website)

## 2.2 Functional Magnetic Resonance Imaging Process

In fMR imaging, the activation in brain in response to a stimuli is measured indirectly. The energy necessity caused by the electrical activity in neurons increases the oxygen level in blood. This rise in oxygen level fades the deoxyhemoglobin concentration in blood. Since deoxyhemoglobin is paramagnetic, it is a factor that makes inhomogeneity in MR signal. The lesser the deoxyhemoglobin amount is in blood, the lesser the inhomogeneity that is observed. Therefore a ratio of 2-4% increment in MR signal can be seen in the activated regions due to reduced inhomogeneity. This blood-oxygen-level dependent (BOLD) process is relatively much slower than the electrical activation. While activation in response to cognitive stimuli can be observed through 100-400 milliseconds via electrical measurements, it can be observed through 6-12 seconds via

BOLD measurement. Hence fMR experiments should be designed considering that the activation can only be predicted in a time frame with 12-15 second resolution.

In fMR experiments, the stimulus is applied consecutively for 5 minutes in order to create BOLD activation continually in related brain regions. As shown in the figure below, 6-10 low resolution whole brain images are acquired during the interval of reaction for each stimulus (12-15 seconds). In this way, BOLD activity created by a single stimulus is stored in multiple 3D image files as intensity.

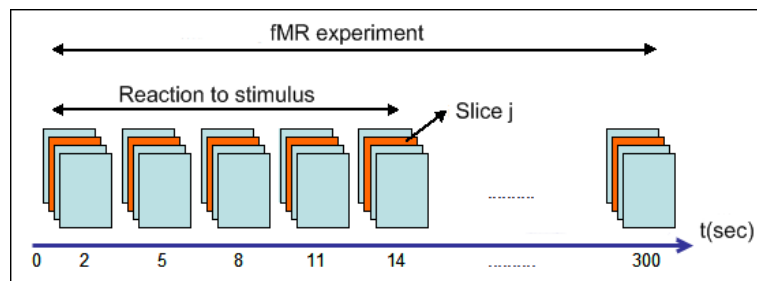


**Figure 2** Typical fMRI experiment

During the analysis, each voxel inside 3D space of the head is individually examined as a time-series of intensities. The intensity value of an activated voxel in time-series seems very different in comparison to a non-active voxel. Generally, only noise can be observed in non-active voxels, while noise plus the reaction to stimulus as an additive 2-4% signal amplitude on top of the baseline DC signal can be found in active voxels.

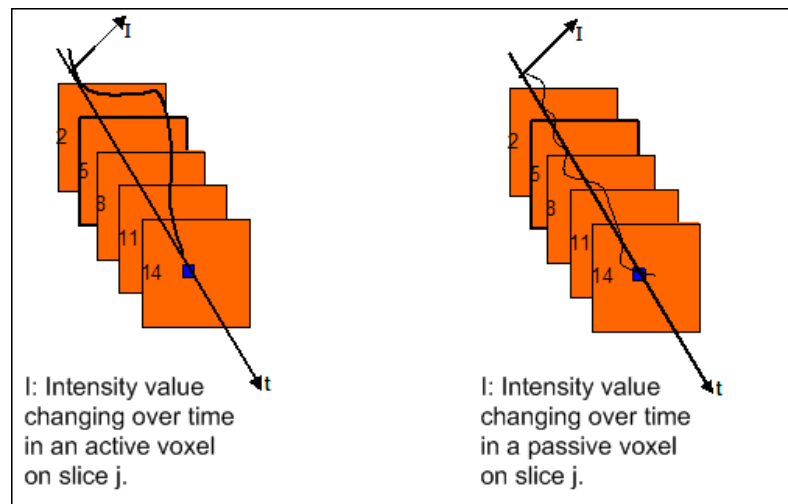


**Figure 3** Intensity change over time in fMRI

## 2.3 fMRI design paradigms

Until now, in literature, two main fMRI design paradigms are exploited: Block and event-related.

### 2.3.1 Block design paradigm

It is expected from the subjects to perform actively a psychological or cognitive condition called as T1. Some regions in the brain of the subject is activated under this condition to do the required operation. This condition should force the subjects to do same operation multiple times along a 15-30 seconds time period, so that a cumulative activation can be observed. After T1 ends, it is desired the subject to perform another condition called T2. T2 has to put the voxels, which are active in T1, in passive state. For example, T1 can be the process of moving fingers and T2 can be rest. In that case, during T1, activity can be monitored in motor cortex and during T2, not such activation is observed. The 3d whole-brain images acquired during the active condition T1 are classified as ON and the images during the passive condition T2 are classified as OFF. T1 and T2 repeat consecutively in time and the images taken during ON and OFF intervals are gathered in two groups representing ON and OFF states. For 1.5T MR

devices, in active voxels, a 1.5-3% signal difference can be monitored between the ON and OFF groups, whereas no significant difference is observed for inactive voxels. At the end of the task, image analysis is done for each voxel. The intensity values of each voxel in different classes (ON and OFF) are compared with a statistical method like t-test or correlation test. If there is a statistical difference between the intensities of conditions, the voxel is accepted as active. For example, a signal acquired from an active voxel in central sulcus during a finger tapping experiment is shown below.

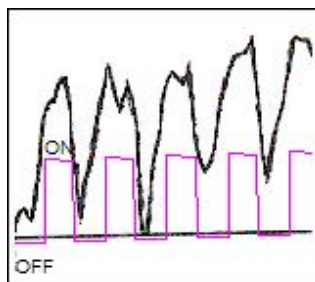


**Figure 4** Finger tapping experiment

### 2.3.2 Event-related design paradigm

The subjects perform only one psychological/cognitive action for each trial. Firstly a stimulus is sent to the subject and a response, such as pressing a button is expected from the subject. Sending stimulus and waiting for a response usually takes 12-16 seconds. During this period, several 3d whole-brain images are acquired as signal samples. In case of activation of a voxel, the signal rises and falls within a time period of 16 seconds, and this type of characteristic activation curve is called HRF (Hemodynamic response function). In multiple brain regions, it is possible to observe delay effects and find regions which are activated earlier than others by observing the lag in the HRF. In this paradigm, the experimental design is more suitable for psychological tasks. However, in active voxels, since there is no cumulative action, the fMR signal difference buried in the hemodynamic response magnitude is barely 0.5-1% in a 1.5T MR device. This makes it difficult to isolate active voxels from inactive voxels. Therefore a lot of stimuli, on the order of 200 need to be tested in order to detect a statistical significance

in the active regions. In figure shown below, an example HRF driven from an active voxel is sketched.

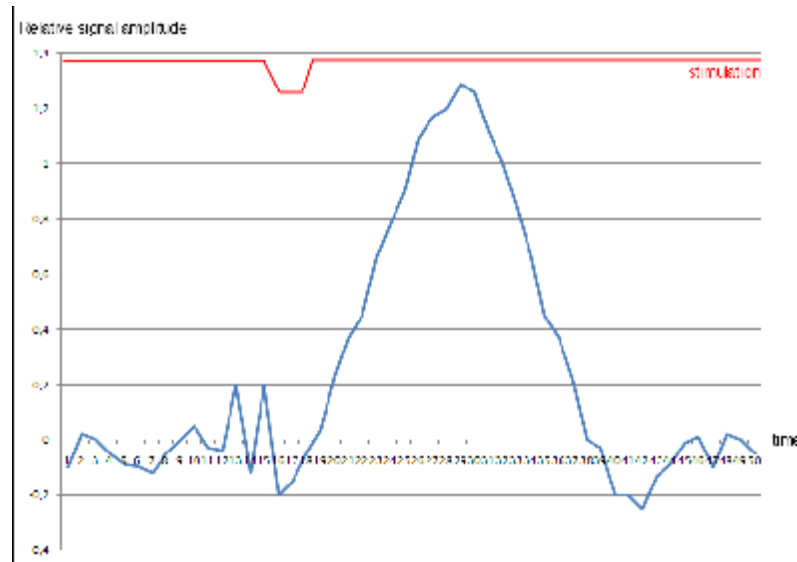


**Figure 5** Hemodynamic response from an activated voxel.

## 2.4 fMRI artifacts

### 2.4.1 Scanner drift

System noise generally describes variations or discrepancies in the functionality of the imaging hardware. Some common causes of system noise are static field inhomogeneities due to imperfect shimming, nonlinearities and instabilities in the gradient fields, and off-resonance or loading effects in the radiofrequency transmitter and receiver coils. Problems with the homogeneity of the main field cause spatial distortions or intensity variations across the images. One particularly important form of system noise is **scanner drift**, which results in slow changes in voxel intensity over time (Huettel, 2004).

Scanner drift is a commonly observed source of low-frequency structured noise in fMRI. It may represent slowly changing local magnetic field strength over the course of the experiment or heating of the equipment over time. It may be due to gradually progressing motion such as subject's head sinking into padding or some other kind of physiologic change. However, the drift is also observed in cadavers and phantoms (Holodny, 2008). Usually this type of signal change can be modeled using first, second or third order polynomials.

#### **2.4.2 Cardiac pulsation**

The physiologic activities of the subject's body can produce structured noise in fMRI experiments. Cardiac and respiratory activity, eye movements, swallowing and usual neural activity can be easily given an example for this type of artifacts. Among these physiologic signal changes, cardiac activity has the highest amplitude and is observed most frequently. The motion of pulsating arteries causes vibration of adjacent structures resulting in signal variation. Additionally, flow artifacts are seen around the vessels. During systole, there is increased blood delivery volume to the brain. Because the cranium is fixed in size, the increase in blood volume causes compression and shifting of the brain (Holodny, 2008).

The regular oscillatory activity of the heart and lungs cause small-scale motion effects in the fMR images. This activity is much faster and more periodic than large-scale head motion, introducing a different set of challenges. If the rate of sampling is fast enough, it may be possible to characterize and minimize motion due to heart and lung activity during preprocessing. But in most fMRI studies, motion due to cardiac activity, in particular, is too fast to be sampled effectively. Due to the time resolution of sampling, respiratory activity may be undersampled. Therefore the resultant effect of cardiac pulsation in fMR images is distributed throughout the fMRI time series in a manner that may be difficult to identify or correct. This type of misattribution of periodic noise sources by undersampling is known as aliasing. Respiration also introduces variability in



the fMRI signal through systematic distortions in the magnetic field. As the subject breathes, the expansion of the lungs casts a magnetic susceptibility “shadow,” influencing field strength and homogeneity of the magnetic field and altering signal intensity throughout the image (Huettel, 2004). Cardiac pulsation can be modeled as a stationary signal at a specific frequency such as 1.5 Hz.

### **2.4.3 Habituation**

Habituation can be considered as some form of learning. The habituation effect occurs when the same stimulus is given repeatedly for an extended time period. The brain area which produces activity in response to the stimulus develops adaptation over time, and the amount of extra oxygen delivered to this area is reduced. This is observed as a decrease in the magnitude of the hemodynamic response. Habituation is considered as a cognitive artifact, unless the experimental paradigm is specifically designed to measure the amount of learning -hence habituation- over time (Holodny, 2008). Habituation can be modeled as a linear loss of signal magnitude.

### **2.4.4 Subject Motion**

Signal variability due to subject motion is common and extremely disruptive for fMRI studies, because it is rarely random. If motion were completely random, then it would introduce noise that reduces SNR but that could be remedied through signal averaging. However, throughout an experiment, a subject may spontaneously shift the position of their head; move their shoulders, arms, or legs to become more comfortable; and swallow or yawn due to nervousness. In the best cases, small head motions may be partially corrected during data preprocessing. However, in the worst cases, large motions may render data completely uninterpretable.

Motion causes problems because of spatial and time-related variability across the set of fMR images. Spatially, motion artifact is not uniform, because a voxel near the edge of the brain, contains mostly cerebrospinal fluid therefore, more prone to movement artifacts. Time-wise, motion is rarely random, and is often correlated with the experimental task. For example, the subjects hold their breath each time they press a response button, or tend to relax and move their heads backward during the rest periods (Huettel, 2004). Motion can be modeled as a rigid transform of each 3D fMR image sample from a specific 3D fMR image sample.

## **2.5 FSL's POSSUM**

POSSUM (Physics-Oriented Simulated Scanner for Understanding MRI) is a software tool for generating simulated MRI and fMRI images and it is a part of FSL (FMRIB's Software Library) (Smith, 2004). POSSUM has tools for MR pulse sequence generation, signal generation, noise addition and image reconstruction that can be managed by the user via a graphical user interface. (Drobnjak, 2006)

As stated in its name, POSSUM is mainly specialized in MRI physics and allows the user to define a lot parameters related to MRI physics. In order to simulate an fMR image, POSSUM relies on the existence of an actual fMRI file, which is obtained earlier. In POSSUM, the fMRI file is only used to augment the simulated MRI.

POSSUM has also an option to add motion to the fMRI experiment, but it produces the motion at specified time points exclusively. There is no chance to produce motion correlated with fMRI design paradigm. Therefore, although it is a useful tool, POSSUM does not allow for generation of fMR activity from scratch. Almost all of the scanner protocol parameters used in POSSUM are adjustable as seen in the figure below. However, there is no specific adjustment for including experimental parameters of the fMRI studies.

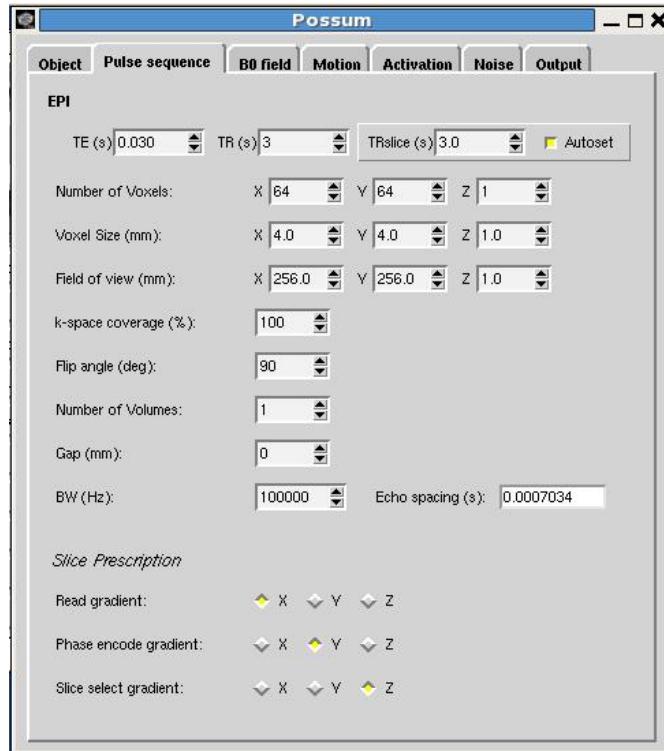


**Figure 6** POSSUM's GUI (<http://www.fmrib.ox.ac.uk/fsl/possum/index.html>)

## CHAPTER 3

### METHODS

#### 3.1 Components Of The METU-fMRISim

Based on a set of artifacts we developed a 3D fMRI simulator, named METU-fMRISim. Our simulator generates fMRI time series at each MRI voxel location, based on parameter settings. The components that constitute the fMRI simulator toolbox are listed in the subsequent sections. Main components are given in the following table.

**Table 1** The main components of the simulator.

Description	Signal
• Simulated anatomic brain volume	
• 4D ideal fMRI time series generation	$f(i)$
• Block paradigm	$b(i)$
• Event-related paradigm	$e(i)$
• Artifacts	
○ Scanner drift	$d(i)$
○ Cardiac pulsation	$p(i)$
○ Habituation	$h(i)$
• Head movement	
○ Task-correlated motion	$M_c$
○ Spontaneous motion	$M_s$

Block and event related paradigms are implemented using an ‘ideal’ block or event-related stimulus series. This ideal series is convolved with a gamma function ( $gm(i)$ ) to reflect the HRF response. The block and event-related paradigm components are centered around a chosen voxel. This voxel is considered to be the focus of activity and immediate neighbors share the activity profile, as dampened by a 3D Gaussian function ( $g_r(i)$ ). On the other hand the artifacts and head movement effects are reflected on the whole 3D fMRI dataset.

The relationship between these components and flow of the simulation process can be seen in figure below.

All components seen in Figure 7 are implemented in the scope of this thesis, except the MINC 2.0 file format input/output routines. MINC 2.0 routines are officially distributed by McConnell Brain Imaging Centre of the Montreal Neurological Institute.

For software development, C++ was chosen as the programming language and the popular cross-platform GUI library Qt was used for handling user inputs and displaying the generated fMRI study. For low level programming issues like threading, memory management etc. , BOOST C++ libraries was used.

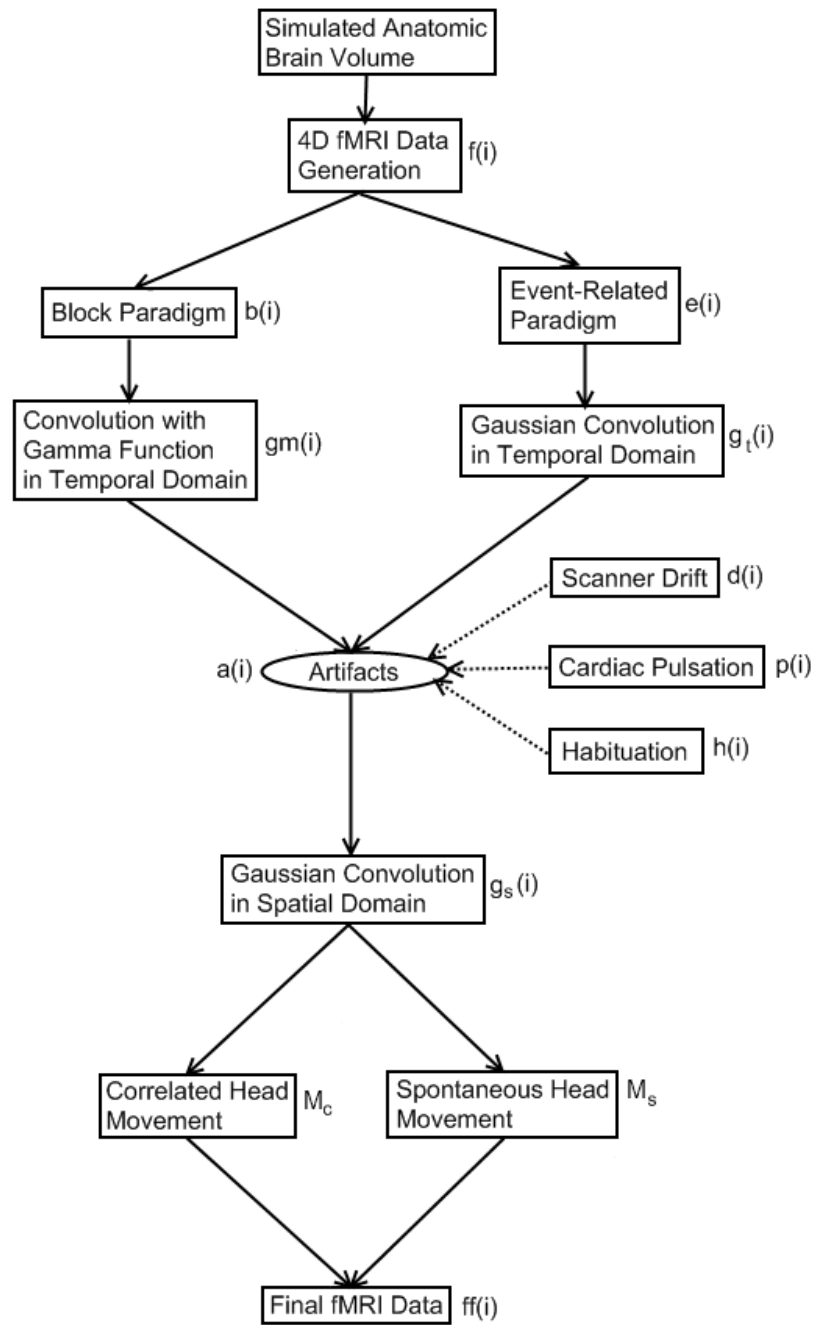


**Figure 7** Components of the simulator.

### **3.1.1 Simulated anatomic brain volume**

Our fMRI simulator reads in an anatomic data and generates fMRI data on this anatomic volume with the experimental settings given by the user.

Montreal Neurological Institute's MRI volume simulator was used to generate the anatomic brain volume. The MRI volume simulator can be found at the following link ([http://mouldy.bic.mni.mcgill.ca/brainweb/selection\\_normal.html](http://mouldy.bic.mni.mcgill.ca/brainweb/selection_normal.html) ). The anatomic volume we used was generated with T1 modality, 1mm of slice thickness, 3% of noise and 20% intensity non-uniformity parameters.

Montreal's simulator gives the results in MINC file format, but before the generated volume is used in our software, it should be converted to MINC 2.0 file format (Baghdadi, 2004). "minconvert" tool, which can be found in MINC binaries, was used for this file format conversion.

#### **The MINC 2.0 File**

MINC was developed by Peter Nellin at the McConnell Brain Imaging Center as a software system for storing and manipulating medical images and allows researchers to use a common set of tools and files to work with medical images in a variety of modalities (Baghdadi, 2004).

The MINC (Medical Imaging NetCDF) 1.0 file format was designed as a file format for medical imaging data building upon the NetCDF (Network Common Data Format) standard (Rew, Davis, 1997) (Baghdadi, 2004). MINC was designed specifically to provide the medical-imaging research community with a modality-neutral way to store medical images along with a rich and flexible set of supporting data.

While the the MINC 1.0 file format has been found to be both powerful and useful over the last decade, a number of limitations have been identified by its users. In particular,

three of these limitations have driven the design of MINC 2.0, the next step in MINC's evolution (Baghdadi, 2004).

- Limited file size
- Restricted data types
- Limited storage options

Since most of these problems were inherent in the MINC 1 file format, it was clear that the design of MINC 2 would require a major revision of the file format. The team developing MINC 2 chose to replace NetCDF with the HDF5 library to form the basis of the MINC 2 format. HDF5 provides a number of advanced features which are not available in NetCDF (Baghdadi, 2004).

In our project, MINC 2.0 libraries and binaries provided by Baghdadi were used in order to read voxel values from the MINC 2.0 file formatted simulated anatomic brain volume.

### **3.1.2 4D fMRI data generation**

An anatomic brain volume should be selected as an underlay to guide fMRI study, and the basic parameters of the fMRI study such as resolution within a slice, number of slices, length of the time series and initial baseline values of the time series, could be easily defined by using the components of this user interface. The study length is based on a generic time unit, which is equivalent to a single TR of the scanner. Once defined, these parameters are held constant throughout all voxels.



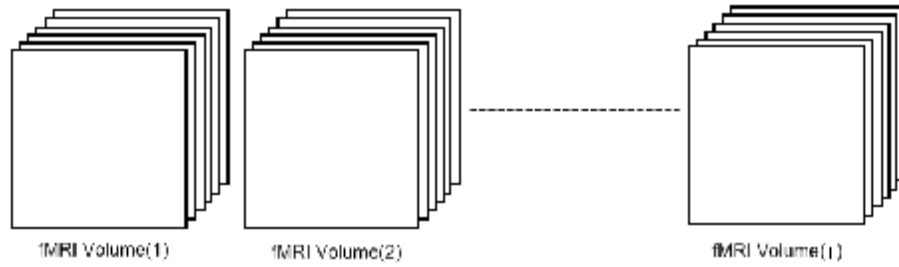


**Figure 8** A study consists of  $i$  volumes.

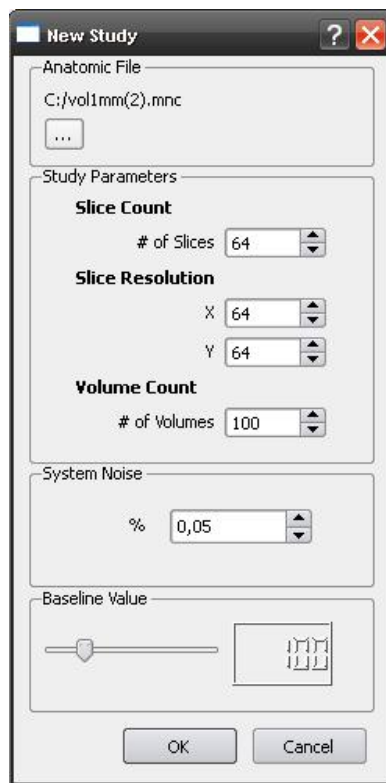


**Figure 9** GUI of the 4D fMRI data generation

The parameters can further be explained as follows:

**Anatomic File:** Anatomic brain volume file in the MINC 2.0 file format.

**Slice Count:** This indicates the number of slices in the study.

**Slice Resolution:** This indicates the number of x and y voxels per slice.

**Volume Count:** Number of samples in time series, or in other words, number of whole brain volumes obtained.

**Baseline Value:** The baseline value,  $f(i)$  (DC component) of the time series in each voxel.

**System noise:** The percent of system noise which will be added to the baseline value.

$$\begin{aligned} f(i) &= V + n(i) \\ n(i) &= \text{random}(n) \end{aligned} \tag{1}$$

Where

$i$  = Index showing of sample points ( $i=1, \dots$ , Volume count)

$V$  = Baseline value.

$n(i)$  = Noise function

$n$  = Maximum amplitude of the noise signal in terms of percent.

### 3.1.3 Block paradigm

The simplest way to evaluate the effect of the independent variable on the dependent variable is to compare an experimental condition to a control condition. Here, the independent variable is the sample-points of the voxel time-series, and dependent variable is the value of the voxel time-series. In order to design a block paradigm, consecutive trials from each condition are grouped together in time to form blocks. Generally, transition between blocks cause changes in the level of an dependent variable. In most fMRI block paradigms, there are two conditions: ON and OFF. In addition, there is also a need to accommodate for 'lag'. When the change of the dependent variable happens not instantaneously at transition of blocks, but after some delay, lag is present.

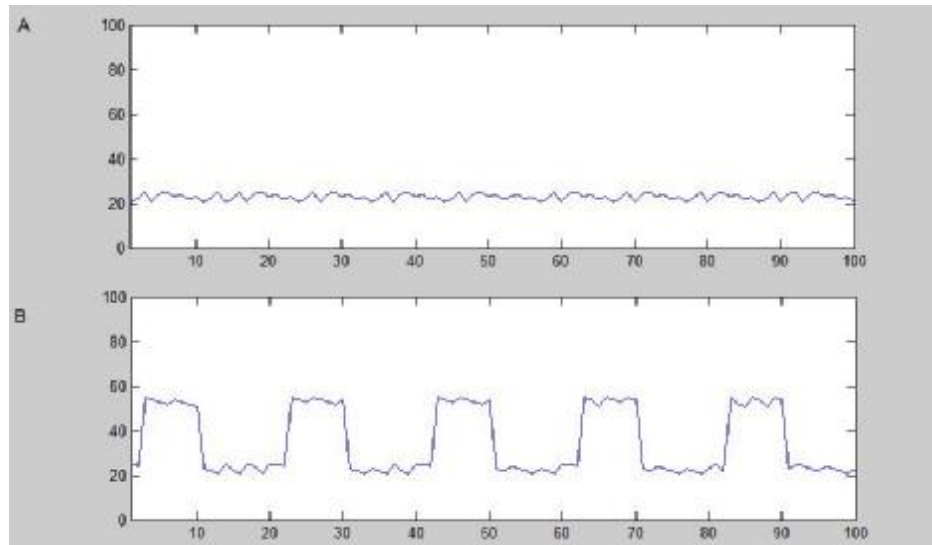


**Figure 10** (A) Initial signal  $f(i)$ , (B) Block paradigm added signal  $b(i)$  with the following parameters: Baseline Value=20; Volume Count=100; Lag=0.

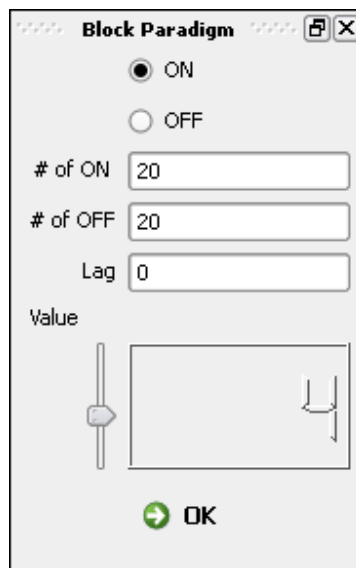


**Figure 11** GUI of block paradigm.

The parameters can further be explained as follows:

**ON/OFF:** The starting state of the block paradigm.

**Number of ON points:** The number of time samples that are bundled together as ON condition.

**Number of OFF points:** The number of time samples that are bundled together as OFF condition.

**Value:** The increased magnitude of the dependent variable during ON condition in terms of percent.

### **Convolution with gamma function in temporal domain**

After the creation of the square wave signal, it is convolved to smooth the edges with gamma kernel, which is produced via gamma distribution.

$$gm(i; k, \theta) = i^{k-1} \frac{e^{-i/\theta}}{\theta^k \Gamma(k)} \quad (2)$$

And

$$\Gamma(k) = (k-1)! \quad (3)$$

Where

$k$  is shape of distribution,  $k > 0$  and accepted as 1 in our calculations  
 $\theta$  is scale of distribution,  $\theta > 0$  and accepted as 1 in our calculations  
 $i$  denotes discrete time points.

**Alternatively**, the Balloon Model (Buxton, 1997) (Buxton, 1998) and the flow-inducing signal model presented in Friston (2000), can also be used at this stage. For the time being, this is planned to be a part of future studies and upgrades.

#### **3.1.4 Event-related paradigm**

The central assumption of an event-related design is that the neural activity of interest will occur for short and discrete stimuli such, as when a brief flash of light evokes

transient activity in the visual cortex. Stimuli that generate such short bursts of neural activity are known as single events or trials. In event related paradigm, the stimuli are given at distinct points of the time-line as impulses. These time points must be specified by the task-designer using a task program synchronized with the sample points. 'Presentation'<sup>1</sup> and 'E-prime'<sup>2</sup> software tools are some programs which can perform this function.

Here in the simulator, we assumed that the sequence of impulses are input to the simulator through a text file.

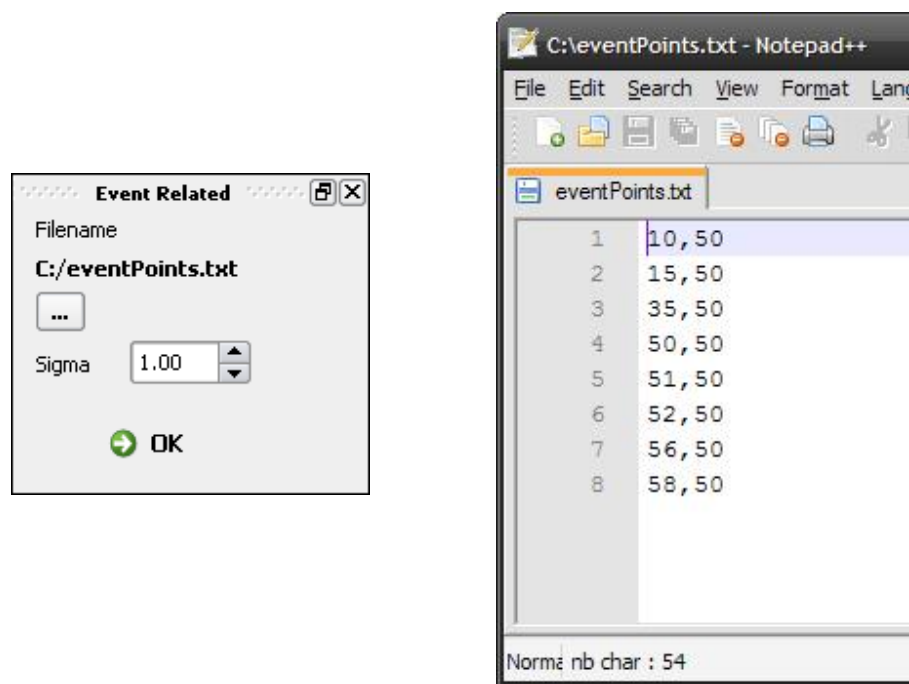


**Figure 12** (Left) GUI of event-related paradigm, (Right) File format of the event points.

<sup>1</sup> Presentation is a stimulus delivery and experimental control program for neuroscience. (<http://www.neurobs.com/>)

<sup>2</sup> E-Prime is a software applications suite for conducting psychological and neuroscientific experiments. (<http://www.pstnet.com/eprime.cfm>)

The parameters involved in event-related time series generation are as follows:

**Event-related filename:** The name of the file which contains the stimulus impulses as indexes of sample points.

**Sigma:** The standard deviation ( $\sigma$ ) parameter of the gaussian distribution for Gaussian convolution explained below.

**Event points:** Index number of the time point at which an impulse occurs. This is indicated in the first column inside the event file.

**Event amplitude:** The signal change (in terms of percent) added on top of the baseline signal as a part of the hemodynamic response. This is indicated in the second column inside the event file.

### Gaussian convolution in temporal domain

For each voxel, the hemodynamic response function (HRF) is thought to be the impulse response function of that location, as illustrated in the figure below.

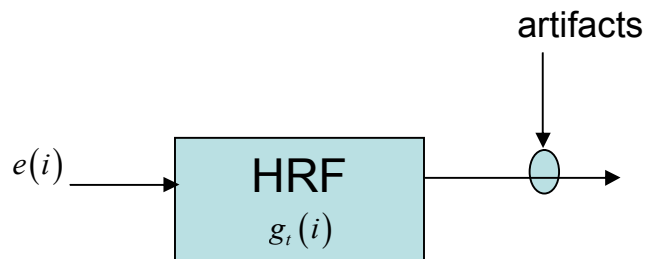


**Figure 13** Impulse response function

Therefore, the observed time-series,  $e(i)$  should be a convolution of the HRF with the specified impulse series,  $f(i)$ . For convolution, a gaussian distribution is chosen to produce an effect like a hemodynamic response. The standard deviation of the gaussian distribution can be manipulated to produce a wide variety of signals. The gaussian function is formulated as:

$$g_i(i) = \frac{e^{-i^2/2\sigma^2}}{\sqrt{2\pi\sigma^2}} \quad (4)$$

Where

$i$  denotes discrete time points.

$\sigma$  is standard deviation.

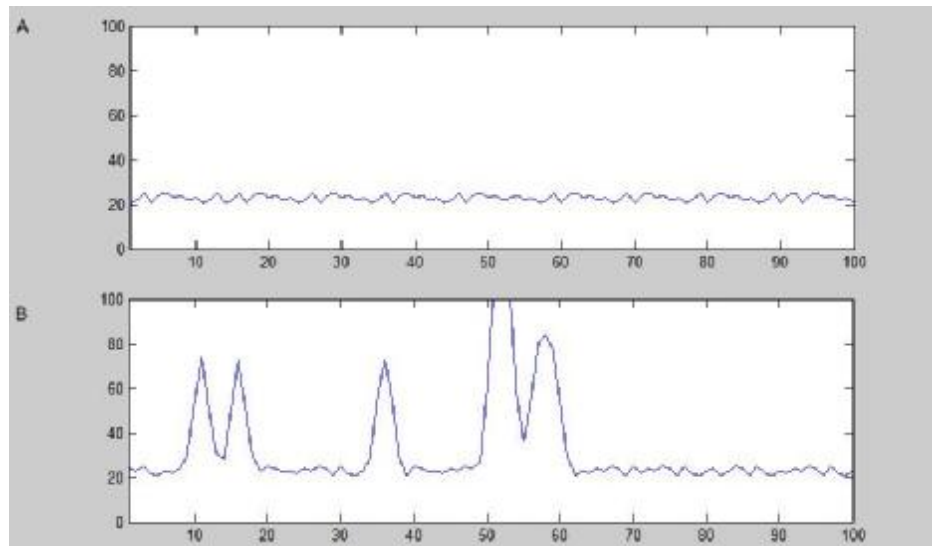


**Figure 14** (A) Initial signal  $f(i)$ , (B) Event-related paradigm added signal  $e(i) * g_i(i)$ .

### Creation of multiple loci:

There is no activation only in one location. Sometimes it is needed to find the relationship of activations from different locations. For that purpose we added a selection mechanism for multiple hot-spots. The paradigms explained till now are generated via the gui shown in figure below.

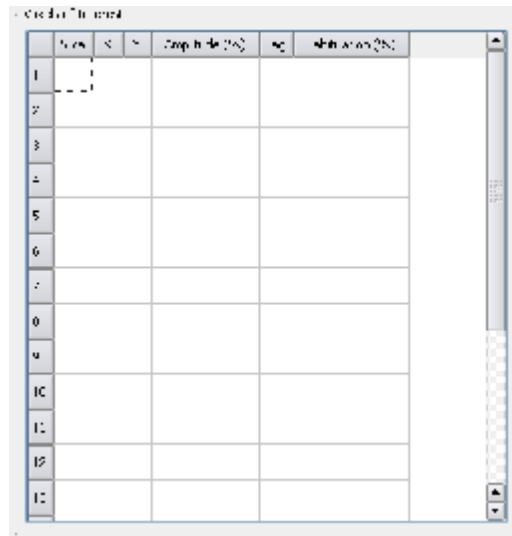


**Figure 15** Multiple hot-spot selection.

**Slice:** The slice of selected voxel.

**X:** The position in the x-axis of the selected voxel.

**Y:** The position in the y-axis of the selected voxel.

**Amplitude:** Signal change amount in terms of percent.

**Lag:** Lag in terms of sample points.

**Habituation:** Explained later in section 3.1.5.3.

The parameters given in this selection GUI is available for both block and event-related paradigms.

### 3.1.5 Artifacts

#### 3.1.5.1 Scanner drift

Scanner drift is an artifact that is caused by the imaging instrument itself. It can be seen as a slight shift of signal along the the study. The magnitude of the signal can be slowly changed over time via adding or subtracting some definite amount,  $a$ , so that this shift can be either in positive or in negative direction.



$$d(i) = i * a \tag{5}$$

Where

$i$  denotes discrete time points.

$a$  is the slope of the drift.

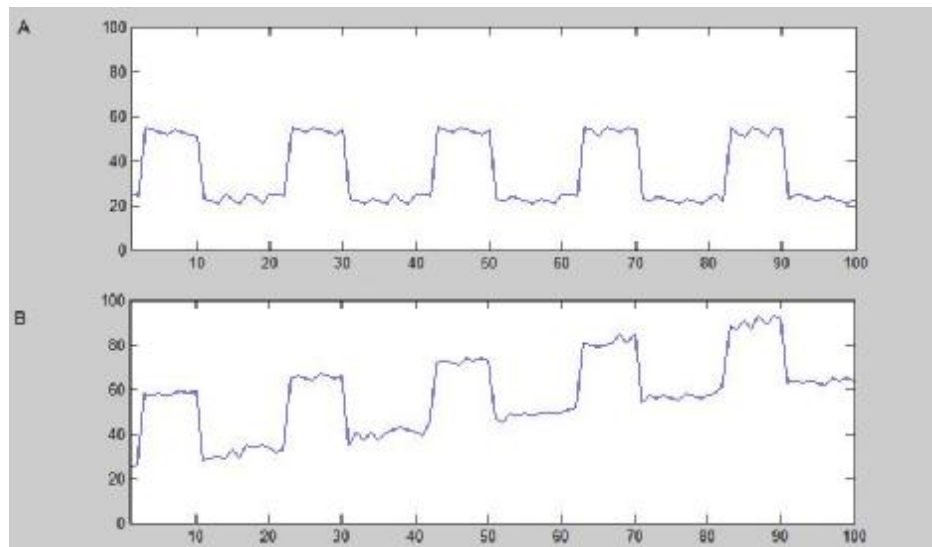


**Figure 16** (A) Block paradigm added signal  $b(i) * g_m(i)$ , (B) After addition of scanner drift  $b(i) * g_m(i) + d(i)$ , where  $a$  is 0.4.

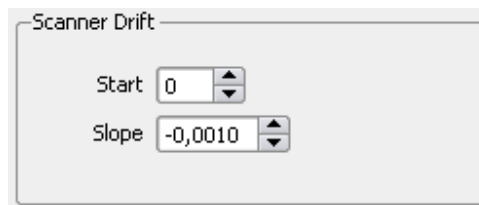


**Figure 17** GUI of scanner drift

The parameters of this operation can be specified as follows:

**Start:** The time point index which indicates the start of the drift

**Drift:** The slope of the drift. It can be either positive or negative. For example, if this value is equal to  $a$ , the signal change will be observed as  $i*a$ , where  $i$  is the independent variable.

Here we have implemented a first order polynomial as drift. In the future we intend to allow for second, third order polynomial drifts as well.

### 3.1.5.2 Cardiac pulsation

The cardiac pulsation is a common artifact in fMRI studies. Every cardiac pulsation makes distortion on the acquired fMRI signal. This can be calculated as:

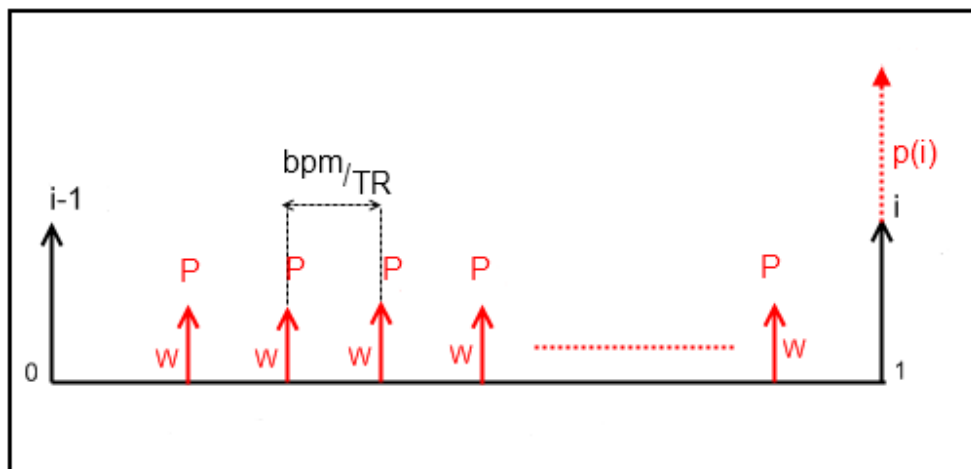


**Figure 18** Pulse sequence between two TRs.

$$p(i) = W * P\# \quad (6)$$

Where;

W is pulse magnitude in terms of percent change.

P# is the number of pulses in 1 TR.

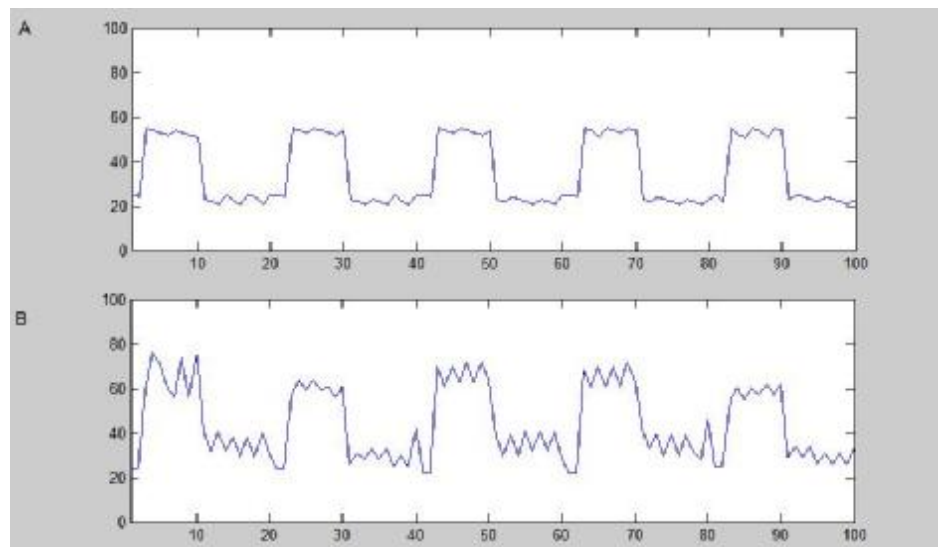


**Figure 19** (A) Block paradigm added signal  $b(i) * g_m(i)$ , (B) After addition of cardiac pulsation  $b(i) * g_m(i) + c(i)$ .

The cardiac effect is added as a percentage of the effected voxel. The amount of percentage is specified again by the user. Time units used here are based on the units specified at the creation of the study.

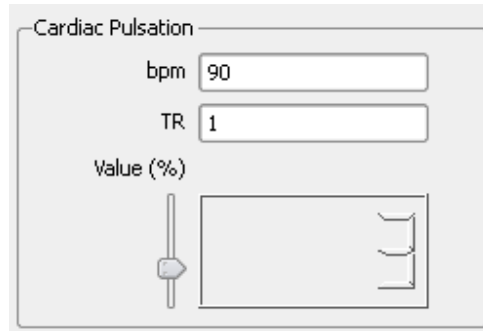


**Figure 20** GUI of cardiac pulsation.

The parameters of this process can further be explained as follows:

**bpm:** The measure of the heart rate, this indicates beats per minute.

**TR:** Repetition time in terms of sample time units.

**Value:** Additive cardiac pulsation value in terms of percent of the current value, this is equivalent to  $W$  in formula 5.

### 3.1.5.3 Habituation

Another artifact in fMRI studies is habituation. It is commonly seen as an attenuation of the hemodynamic response along the timeline, usually corresponding to a diminishing cognitive trend. It can be expressed as a first order equation and the user can change the amount of loss ratio of the signal at the end of the study.

$$h(i) = mi + n \tag{7}$$

Where;

$i$  denotes the time points.

$m$  denotes the slope.

$n$  denotes the starting sample for habituation process, currently this is set to 0.

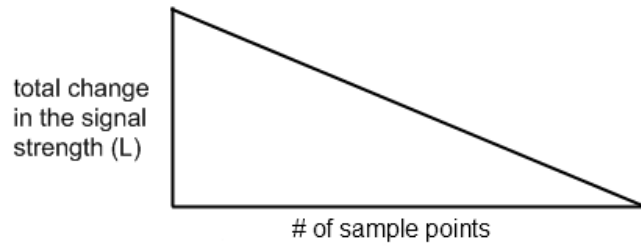


**Figure 21** Loss ratio (slope)

$$m = \frac{-L}{\# \text{ of sample points}} \quad (8)$$

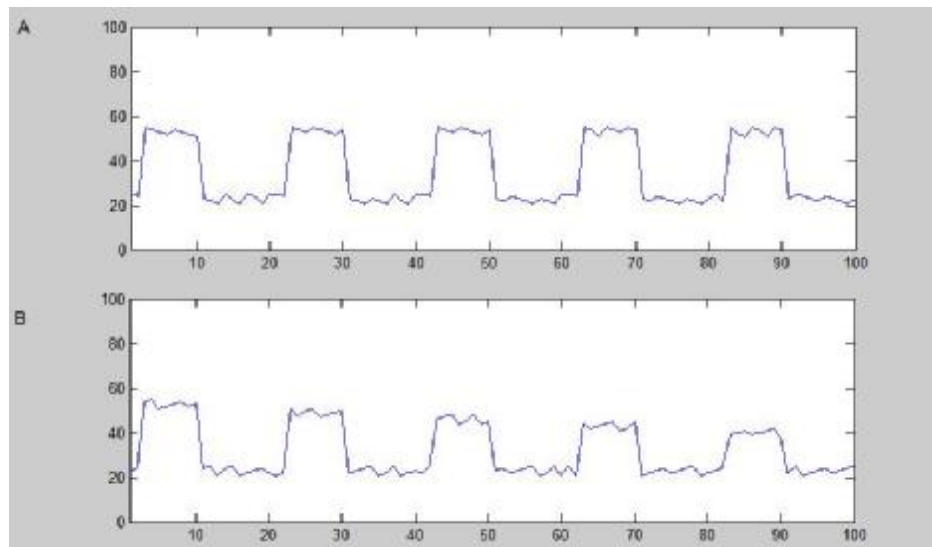


**Figure 22** (A) Block paradigm added signal  $b(i) * g_m(i)$ , (B) After addition of habituation  $b(i) * g_m(i) + h(i)$ , where  $m$  is 0.1

The parameter to be adjusted here corresponds to:

**Loss ratio:** The loss ratio (L) in hemodynamic response during the whole fMRI experiment. This is given in terms of percent and can be entered using the GUI shown in figure 15.

### 3.1.6 Optional gaussian convolution in spatial domain

When a change occurs in the signal magnitude of a voxel, this change may also be reflected to the neighbours of that voxel. In order to achieve this, a 3x3x3 volumetric neighbourhood of the voxel is convolved with a 3x3x3 gaussian kernel, which is acquired with the given standart deviation value in the GUI. The kernel used for the convolution process is generated using the formula:

$$f(x, y, z) = e^{-\left(\frac{(x-x_0)^2}{2\sigma_x^2} + \frac{(y-y_0)^2}{2\sigma_y^2} + \frac{(z-z_0)^2}{2\sigma_z^2}\right)} \quad (9)$$

Where;

$(x_0, y_0, z_0)$  is the spatially middle point of the region, representing the active voxel.

$(x, y, z)$  is within the 3x3x3 spatial neighbourhood of  $(x_0, y_0, z_0)$

$\sigma_x, \sigma_y, \sigma_z$  denotes the variances of gaussian distribution respectively in the x, y and z directions.

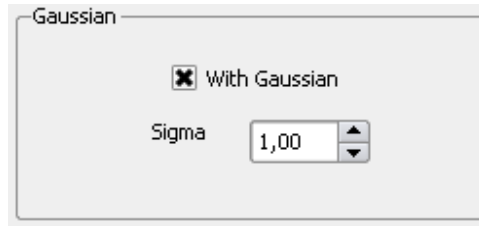


**Figure 23** GUI of gaussian convolution in spatial domain

The adjustable parameter at this stage is:

**Sigma:** The standard deviation value of the Gaussian distribution in terms of voxels.

As seen from here, all  $\sigma_x$ ,  $\sigma_y$ ,  $\sigma_z$  are equal.

### 3.1.7 Correlated head movement

During an fMRI study, the subject's head motion is a commonly seen artifact. While the subject is responding to the given stimuli, there is always a possibility to move or rotate its head in terms of millimeters, even though it is stabilized as good as it could be.

There are two possibilities for head movement artifact. The first possibility is correlated head movement and it is only available for block paradigm fMRI study. Correlated head motion occurs when a stimulus is present. In block paradigm, it is triggered with the first point of the stimulus and every rise of the stimulus in the block design causes the motion again.

This motion can be expressed as the translation, or rotation in 3D space. The new position of every voxel  $(x', y', z')$ , that belongs to MRI volume, is calculated using affine transformation as follows;

$$\begin{bmatrix} X' \\ Y' \\ Z' \end{bmatrix} = \begin{bmatrix} X \\ Y \\ Z \end{bmatrix} + \begin{bmatrix} X_T \\ Y_T \\ Z_T \end{bmatrix} + S * R(\alpha_1, \alpha_2, \alpha_3) * \begin{bmatrix} X \\ Y \\ Z \end{bmatrix} \quad (10)$$

$$(X, Y, Z) \xrightarrow{M} (X', Y', Z')$$

$$M : R^3 \rightarrow R^3$$

Where;

$$\begin{bmatrix} X \\ Y \\ Z \end{bmatrix} \text{ denote the coordinates of the point before motion}$$

$$\begin{bmatrix} X' \\ Y' \\ Z' \end{bmatrix} \text{ denote the coordinates of the point after motion}$$

$$\begin{bmatrix} X_T \\ Y_T \\ Z_T \end{bmatrix} \text{ denote the three translation parameters of motion}$$

$\alpha_1, \alpha_2, \alpha_3$  denote the three rotation angles around the x-, y- and z-axis respectively;

S denotes a scale factor (in our case, it is always equal to 1);

R denote the total rotation matrix which is the product of three individual rotation matrices:



$$\mathbf{R}_{3 \times 3} = R(\alpha_1, \alpha_2, \alpha_3) = R_3(\alpha_3) * R_2(\alpha_2) * R_1(\alpha_1) \quad (11)$$

$$= \begin{bmatrix} \cos \alpha_3 & \sin \alpha_3 & 0 \\ -\sin \alpha_3 & \cos \alpha_3 & 0 \\ 0 & 0 & 1 \end{bmatrix} * \begin{bmatrix} \cos \alpha_2 & 0 & -\sin \alpha_2 \\ 0 & 1 & 0 \\ \sin \alpha_2 & 0 & \cos \alpha_2 \end{bmatrix} * \begin{bmatrix} 1 & 0 & 0 \\ 0 & \cos \alpha_1 & \sin \alpha_1 \\ 0 & -\sin \alpha_1 & \cos \alpha_1 \end{bmatrix}$$

$$= \begin{bmatrix} \cos \alpha_2 \cos \alpha_3 & \cos \alpha_1 \sin \alpha_3 + \sin \alpha_1 \sin \alpha_2 \cos \alpha_3 & \sin \alpha_1 \sin \alpha_3 - \cos \alpha_1 \sin \alpha_2 \cos \alpha_3 \\ -\cos \alpha_2 \sin \alpha_3 & \cos \alpha_1 \cos \alpha_3 - \sin \alpha_1 \sin \alpha_2 \sin \alpha_3 & \sin \alpha_1 \cos \alpha_3 + \cos \alpha_1 \sin \alpha_2 \sin \alpha_3 \\ \sin \alpha_2 & -\sin \alpha_1 \cos \alpha_2 & \cos \alpha_1 \cos \alpha_2 \end{bmatrix}$$

For correlated head movement, all the parameters should be entered via the user interface.

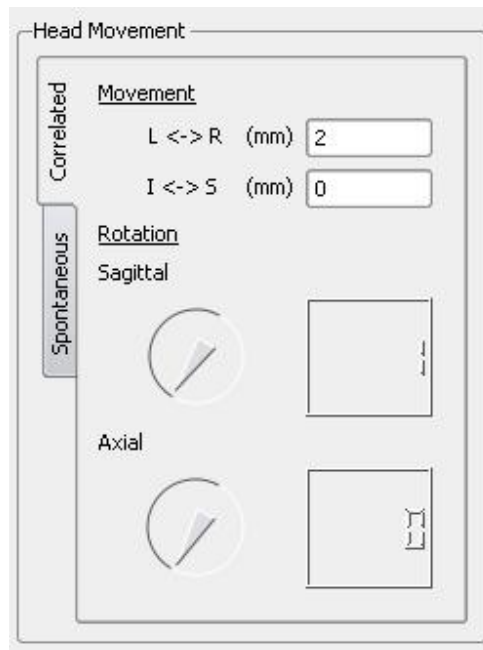


**Figure 24** GUI of correlated head movement

The parameters of this operation can be specified as follows:

**Movement L<->R:** The translation amount in the left-right direction in terms of millimeters.

**Movement I<->S:** The translation amount in the inferior-superior direction in terms of millimeters.

**Rotation Sagittal:** The rotation amount within the sagittal plane.

**Rotation Axial:** The rotation amount within the axial plane.

Coronal rotation is less likely to happen, therefore not implemented here. We will add it in the future versions of METU-fMRISim.

For a visual presentation of anatomical directions and planes, see Appendix A.1

### **3.1.8 Spontaneous head movement**

The second possibility of the head movement is spontaneous head movement and it is available for both block and event-related paradigms. Spontaneous head movement occurs when there is a sudden jerk of the head, for example when the subject sneezes or swallows. It uses the same formulation with correlated head movement, but the input parameters should be given in a formatted text file. Its format is shown below where the 5 parameters indicate sample Time point of motion, left-right translation in terms of mm, inferior-superior translation, sagittal rotation and axial rotation in terms of degrees. By entering multiple lines in the text file, multiple spontaneous motions can be generated.

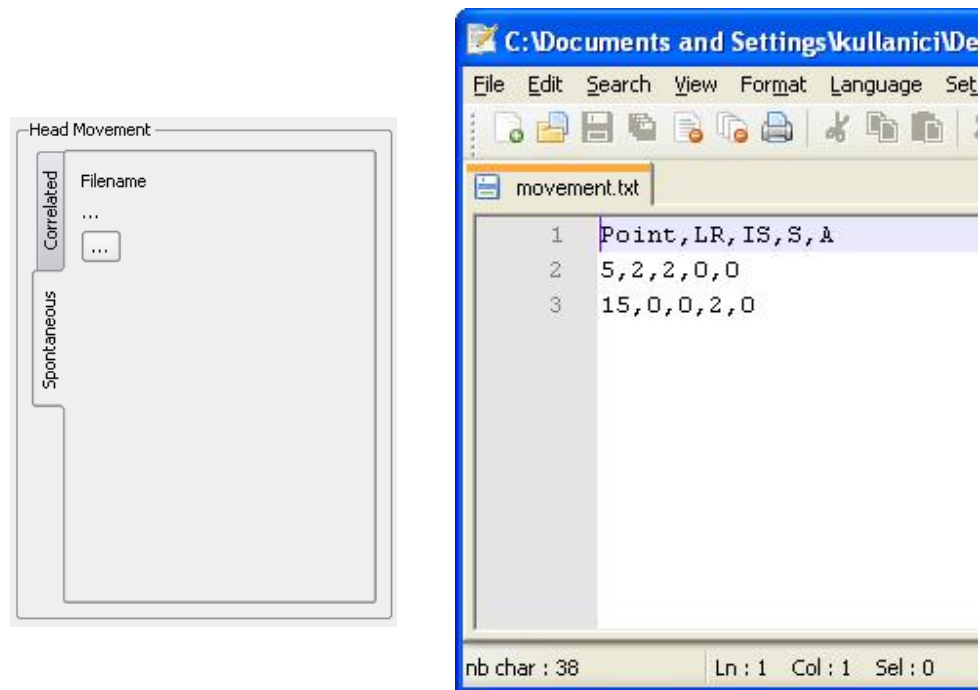


**Figure 25** (Left) GUI of spontaneous head movement, (Right) File structure for spontaneous head movement.

The parameters involved in spontaneous head movement generation are as follows:

**Filename:** The name of the file which contains the points at which a head motion occurs.

**Point:** The time point  $i$ , when a head motion occurs. This is indicated in the first column of the file.

**LR:** Translation amount in the left-right direction in terms of millimeters. This is indicated in the second column of the file.

**IS:** Translation amount in the inferior-superior direction in terms of millimeters. This is indicated in the third column of the file.

**S:** Rotation amount around the sagittal axis. This is indicated in the fourth column of the file.

**A:** Rotation amount around the axial axis. This is indicated in the fifth column of the file.

### 3.1.9 Final fMRI data

The fMRI signal which reflects all the noise and artifact factors described in the previous sections is obtained as follows:

$$ff(i) = M \left\{ [f(i) + z(i) + d(i) + p(i) + h(i)] * g_s(i) \right\} \quad (12)$$

$$z(i) = \begin{cases} b(i) * gm(i) & \text{for block paradigm} \\ e(i) * g_t(i) & \text{for event related paradigm} \end{cases} \quad (13)$$

Where;

$b(i)$  is block paradigm;

$gm(i)$  is gamma function;

$e(i)$  is event-related paradigm;

$g_t(i)$  is gaussian convolution in temporal domain;

$d(i)$  is scanner drift;

$p(i)$  is cardiac pulsation;

$h(i)$  is habituation;

$g_s(i)$  is gaussian convolution in spatial domain;

M is motion;

$ff(i)$  is the final generated data.

The full image of the GUI is seen in the figure below, identifying the settings.

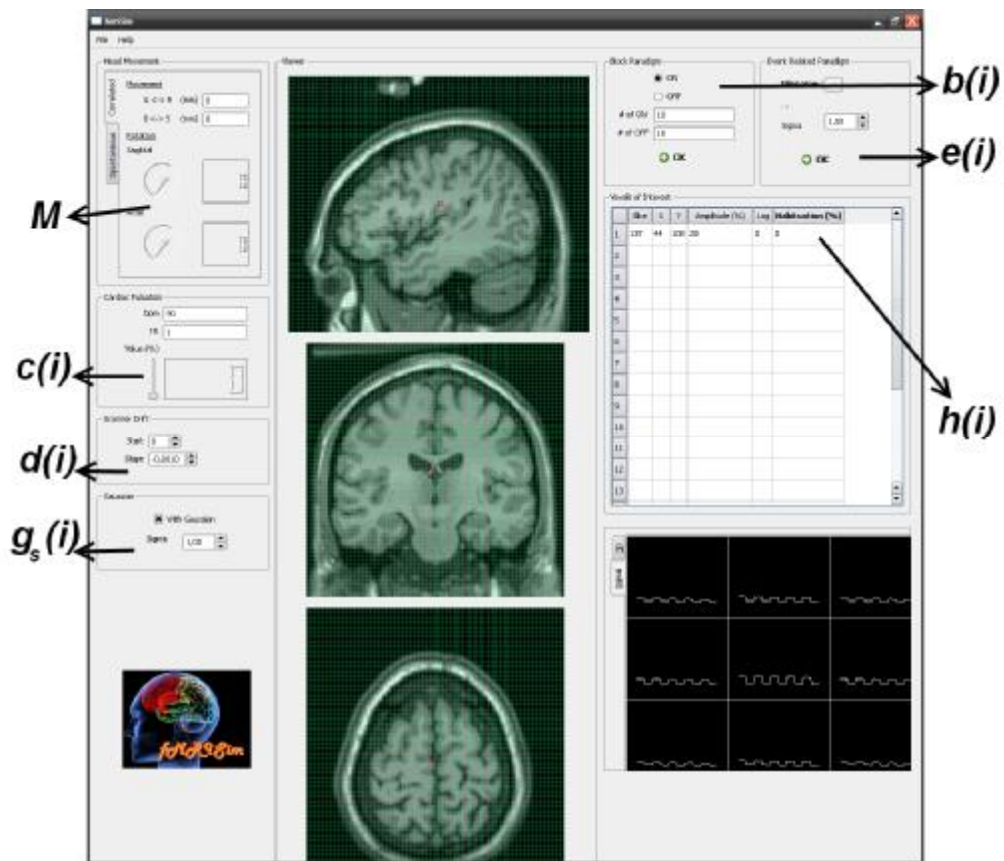


**Figure 26** The main GUI of the simulator.

Once all the activity spots and artifacts are generated, the fMRI time series can be saved using ANALYZE 7.5 file format for being input to other popular MRI software packages like AFNI, FSL and other new fMRI analysis tools.

### **The ANALYZE 7.5 File Format**

Analyze is an image processing program, written by The Biomedical Imaging Resource at the Mayo Foundation. The Analyze data format is used by the Analyze program, and now by a wide variety of other software (<http://imaging.mrc-cbu.cam.ac.uk/imaging/FormatAnalyze>).

There are two Analyze formats. Analyze 7.5 is much more commonly used. An Analyze 7.5 format image consists of two files, an image and a header file. These files have

same name being distinguished by the extensions .img for the image file and .hdr for the header file (<http://eeg.sourceforge.net/ANALYZE75.pdf>). So, for a brain image named brain00, there are two files named as brain00.img and brain00.hdr.

### **Image File**

Image file usually contains uncompressed pixel data for the image in several pixel formats and its format is very simple (<http://eeg.sourceforge.net/ANALYZE75.pdf>).

### **Header File**

The header file describes the dimensions and history of the pixel data and consists of three substructures. (<http://eeg.sourceforge.net/ANALYZE75.pdf>)

- header\_key, which describes the header.
- image\_dimension, which describes the image sizes.
- data\_history, which is optional.

All ANALYZE 7.5 input/output (IO) routines used in this thesis, were written as a part of this thesis, any other third party libraries were not used for Analyze 7.5 IO.

## **CHAPTER 4**

### **RESULTS**

In fMRI analysis there are several software tools which are mostly used such as AFNI, FSL, SPM. These softwares use General Linear Model in order to analyze the fMRI dataset. In our tests, we preferred using AFNI.

AFNI (Analysis of Functional Neuroimages) (<http://afni.nimh.nih.gov/afni/>) is an open source environment for processing and displaying fMRI data. AFNI runs under many UNIX-like operating systems. AFNI is a group of programs that can be used interactively or through batch processing with shell scripts. AFNI is actively developed by the NIMH Scientific and Statistical Computing Core and its capabilities are continually expanding.

In figure shown below, a real MRI is shown via AFNI.

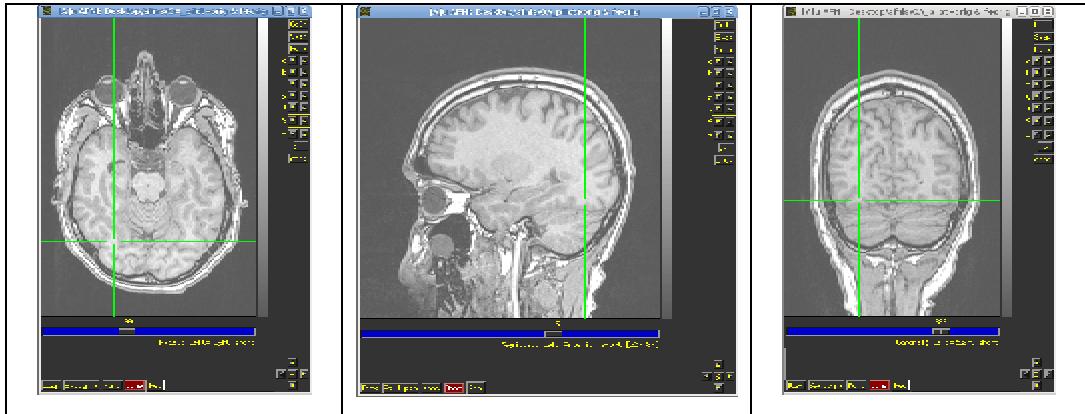


Figure 27 Real MR data.

The fMRI time series at the voxel indicated by arrow in Figure 28 is shown as follows.

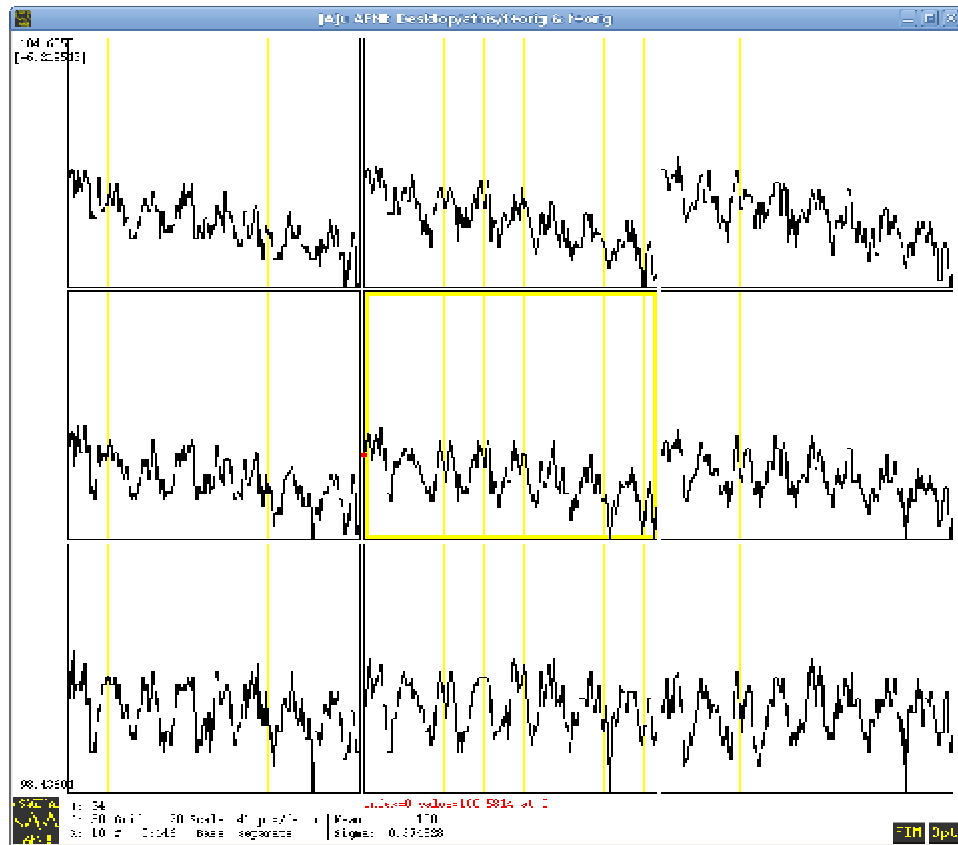
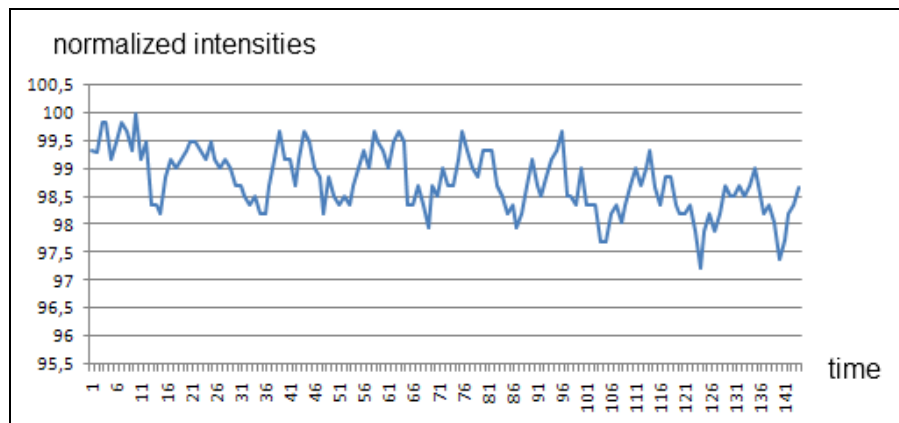


Figure 28 Time series of selected voxel.



#### 4.1 Artifact tests

In order to verify the fMRI artifacts, we have chosen a voxel point from a real fMRI study, and accepted its time series along the whole study as the groundtruth data. The design parameters of that study were as follows: A block paradigm with 9 samples per block and 8 repetitions of each cycle. During the ‘ON’ blocks, face images are shown to the subject and during the ‘OFF’ blocks, scrambled masks are shown. A sample activation site detected by AFNI’s general linear model analysis is shown below in Figure 29 through its time series. We then simulated 4 datasets based on task parameters, all simulated datasets have a baseline value of 99 and a signal amplitude of 1% of the baseline value, while first dataset ( $S_a$ ) has no scanner drift, second dataset ( $S_b$ ) has a scanner drift with -0.0005 of slope value, and third sample ( $S_c$ ) has a drift value of -0.0002. Fourth dataset has same block design parameters and cardiac pulse with 90 bpm, 1TR, 1% percent signal change, and 0.02% habituation (Figure. 30 - 33). The parameters used in simulating datasets were found with trial and error method.



**Figure 29** The groundtruth data. (O)

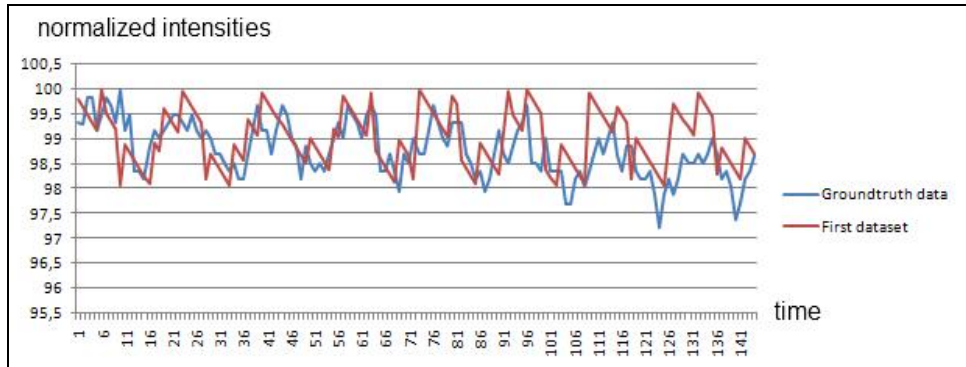


**Figure 30** First simulated data ( $S_a$ ).

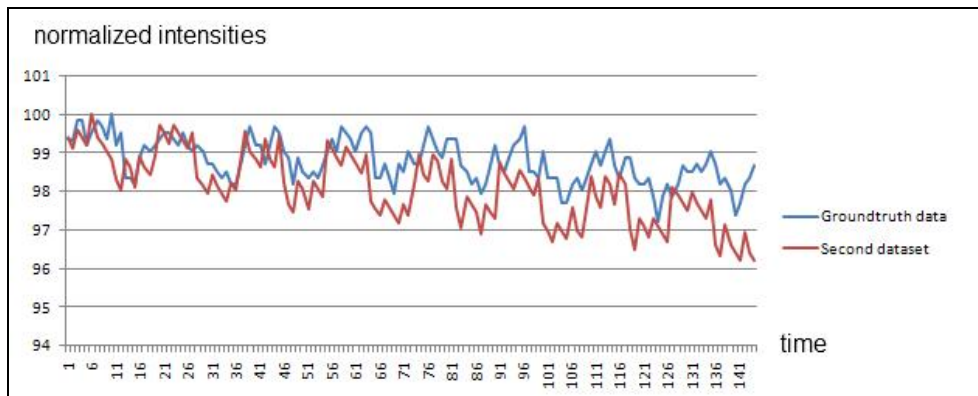


**Figure 31** Second simulated data ( $S_b$ ).

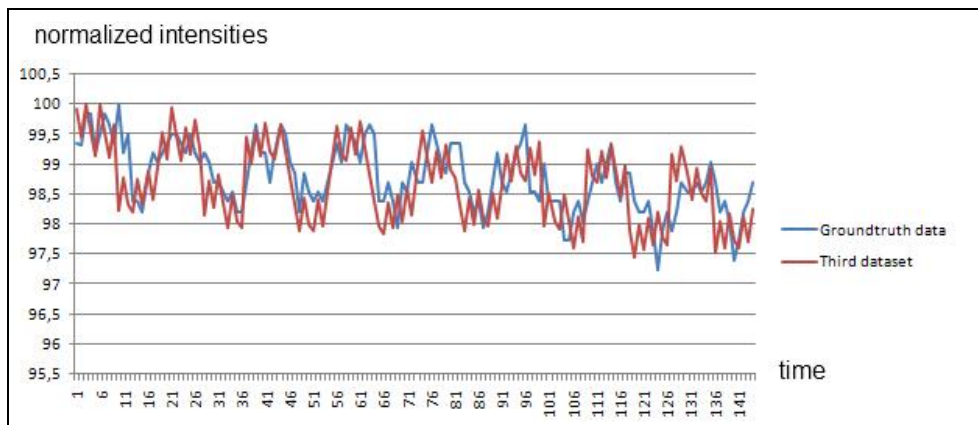


**Figure 32** Third simulated data ( $S_c$ ).

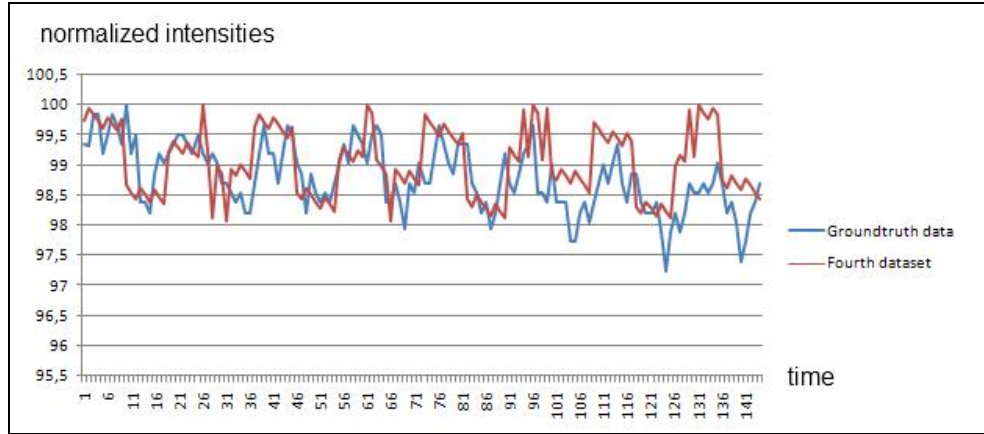


**Figure 33** Fourth simulated data ( $S_d$ ).

In order to show the similarity of the data produced by the simulator to the real data, we used root mean square error.

**Root mean square error:**

The root mean square deviation (RMSD) or root mean square error (RMSE) is a frequently-used measure of the differences between values predicted by a model or an estimator and the values actually observed from the thing being modeled or estimated. RMSD is a good measure of accuracy. These individual differences are also called residuals, and the RMSD serves to aggregate them into a single measure of predictive power.

The RMSD of an estimator with respect to the estimated parameter  $\theta$  is defined as the square root of the mean squared error MSE:

$$RMSD = \sqrt{MSE} \tag{14}$$

$$MSE(O, S) = \frac{1}{n} \sum_{i=1}^n (O_i - S_i)^2 \tag{15}$$

$$RMSD(O, S) = \sqrt{\frac{\sum_{i=1}^n (O_i - S_i)^2}{n}} \quad (16)$$

Where

n : number of time points

O : real time series data

S : simulated time series data

And the the calculated RMSDs;

$$RMSD(O, S_1) = 0.630268$$

$$RMSD(O, S_2) = 0.942751$$

$$RMSD(O, S_3) = 0.523551$$

$$RMSD(O, S_4) = 0.622132$$

The purpose of those tests is not to estimate the amount of cardiac pulse or habituation in the real data. It purely measures that our data generation process is close to the real life fMRI time series. For example, same real life data can be obtained with different combination of drift, cardiac pulsation, habituation parameters, and this does not present a problem on our side.

## 4.2 Motion tests with AFNI

In the order to verify the generated motion, we used AFNI' s **3dvolreg** tool, which stands for 3d volume registration. This tool corrects series of whole brain fMR images for motion and plots motion parameters which are detected. During this process, firstly the fMR image sample which serves as a reference is indicated. All the other 3D image files are treated as samples to be registered with this volume. By comparing all these

fMRI volumes, **3dvolreg** acquires a motion characteristics along all 3 axes and all 3 rotational planes.

In order to test validity of the motion introduced by our simulator toolkit, we initially generated two fMRI datasets with different no motion characteristics, as follows:

- The parameters of **first** dataset are;  
Block paradigm starting ON state with 10 ON and 10 OFF states, no lag and 10% amplitude;  
No gaussian convolution in spatial domain.
- The parameters of **second** dataset are;  
Block paradigm starting ON state with 10 ON and 10 OFF states, 2 time point lag and 10% amplitude;  
Gaussian convolution ( $\sigma = 1$ ).

Then 3dvolreg is used to estimate the motion in those datasets.

For example, the figure below was obtained as the output of **3dvolreg**. In this sample, which represents the first dataset, there was block design paradigm but no head motion. In this graphic(Figure 34),  $\Delta A - P$  indicates the motion estimation along the anterior-posterior axis. The x-axis in the figure shows the sample points in time series. The y-axis shows possible motion in the anterior-posterior direction in terms of millimeters.  $\Delta L - R$  indicates the motion estimation along the left-right axis. The x-axis in the figure shows the sample points in time series. The y-axis shows possible motion in the left-right direction in terms of millimeters.  $\Delta I - S$  indicates the motion estimation along the inferior-superior axis. The x-axis in the figure shows the sample points in time series. The y-axis shows possible motion in the inferior-superior direction in terms of millimeters. The variation in the signal is about 0 for all the parameters. It can be easily seen there is no head motion.

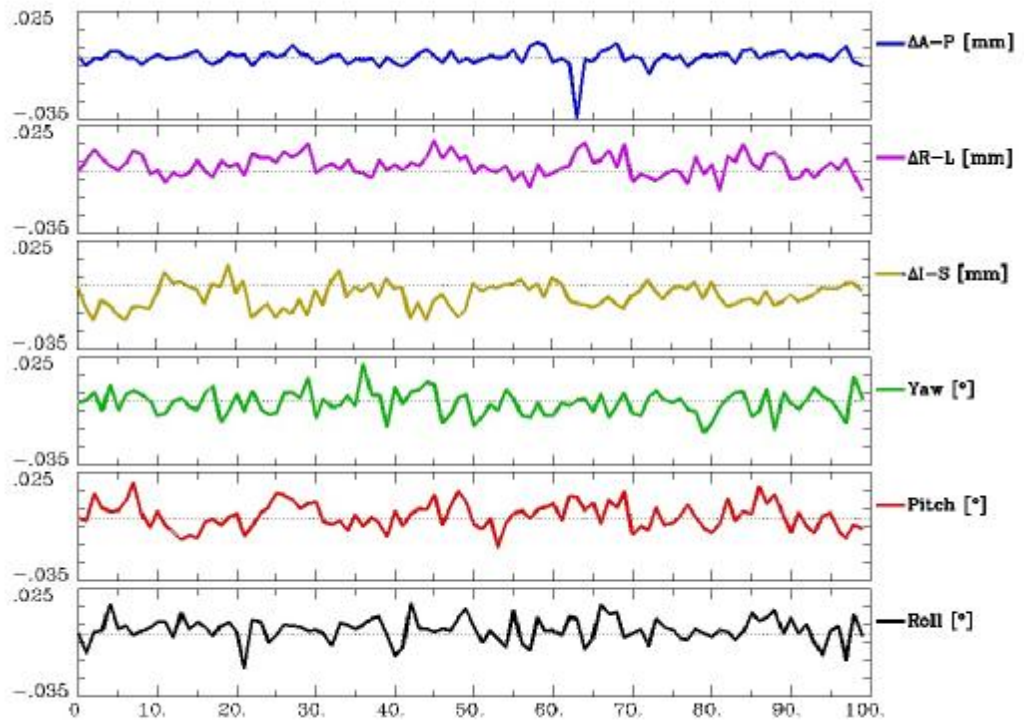


**Figure 34** The motion components of the **first** data (without motion) where the first 3 rows indicate translation in mm and last 3 rows indicate rotation along 3 axes in degrees.

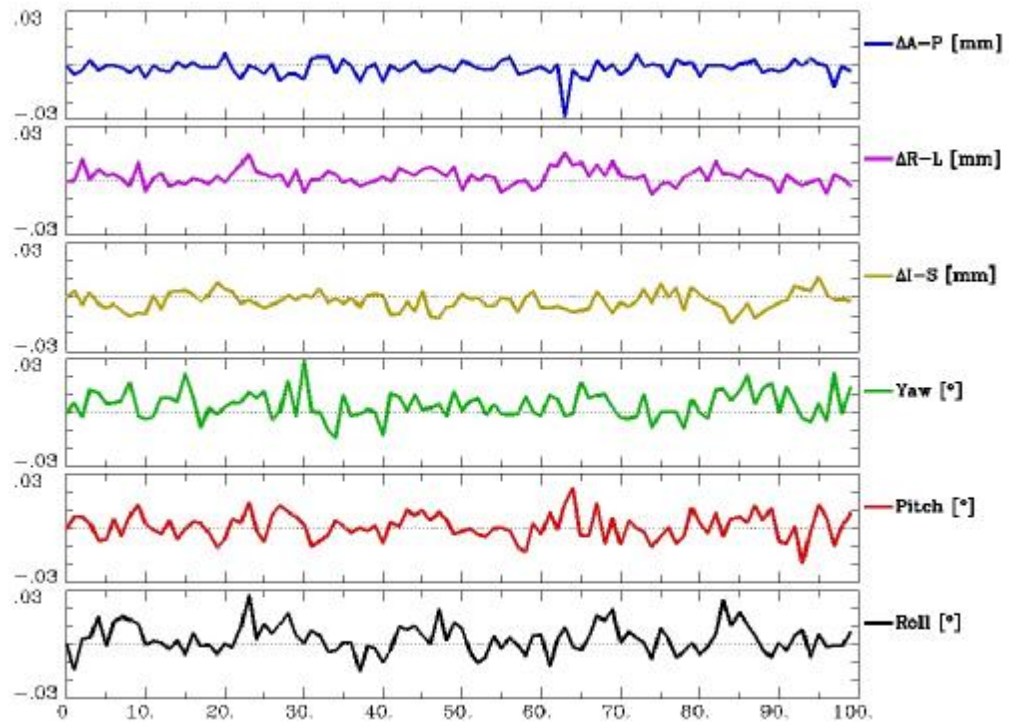


**Figure 35** The motion components of the **second** data (without motion)

Similarly, in figure 35, the y-axis indicates negligible motion estimation, verifying that when there is no motion in presence of other artifacts, AFNI does resolve the time series correctly. In the second phase of our motion tests, we simulated 2 fMRI datasets with correlated motion using METU-fMRISim. The two datasets created before, first and second are used again with different motion characteristics. For the first dataset there was head motion with the following parameters;

- 1 mm translation in the left-right direction (L),
- 1 mm translation in the inferior-superior direction (S),
- 1° of rotation in the sagittal plane.

For the second dataset there was head motion with the following parameters;

- 2 mm translation in the left-right direction,
- -1 mm translation in the inferior-superior direction,
- No rotation.

As shown in the figures below, for first and second datasets we can see the motion components with very close values.

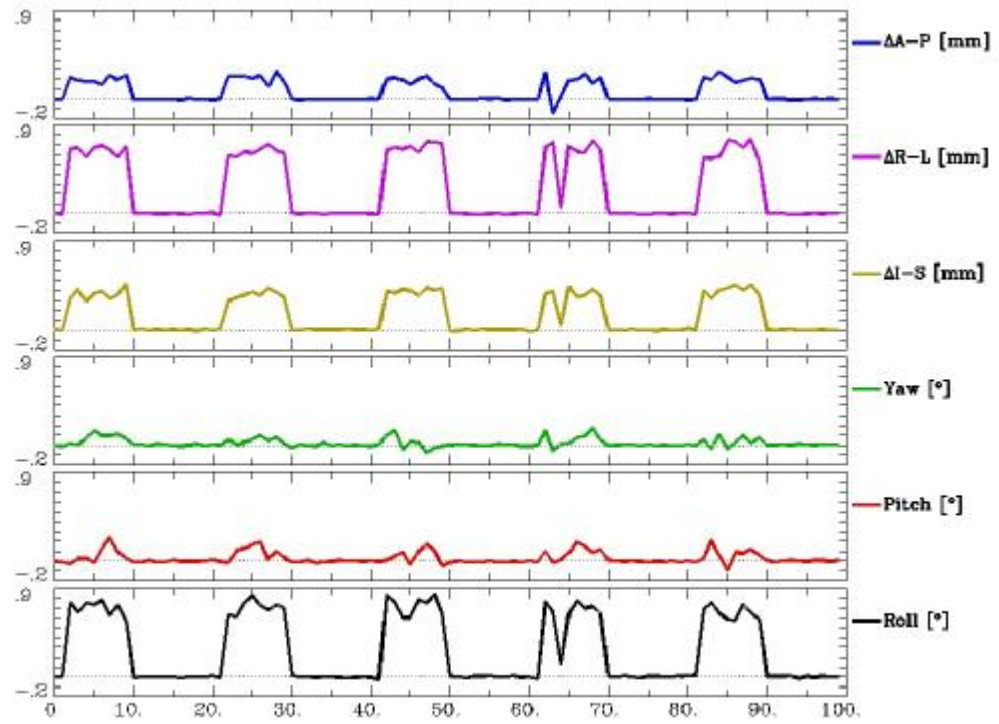


**Figure 36** The motion components of the **first** data (with motion)



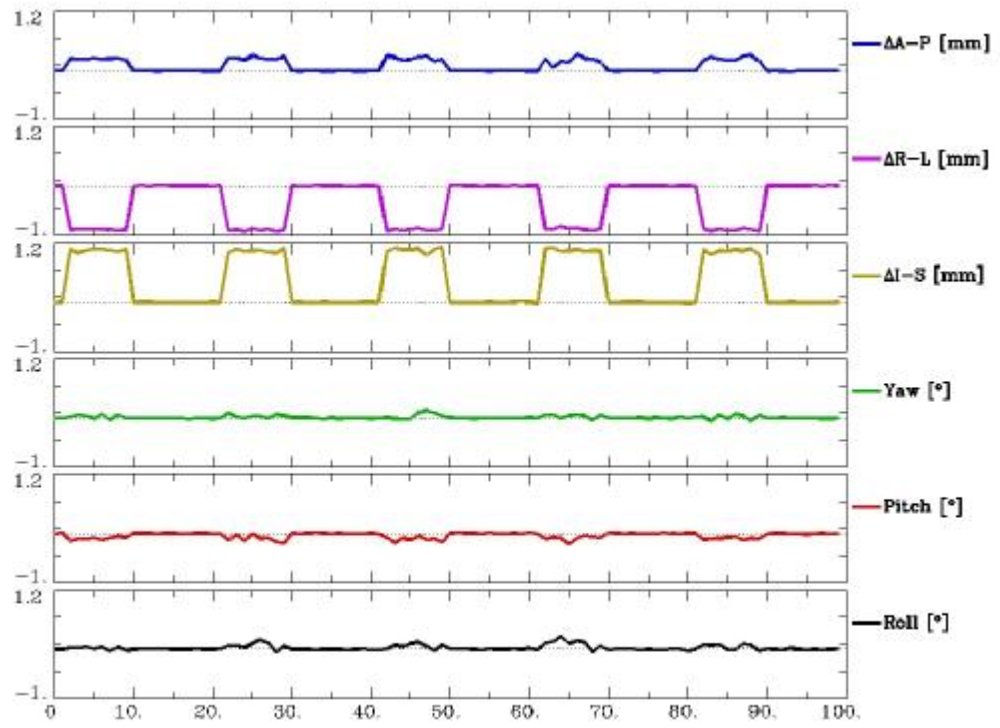


**Figure 37** The motion components of the **second** data (with motion)

## **CHAPTER 5**

### **CONCLUSION**

We implemented a simulation toolkit for generating artificial 4D fMRI datasets. The basic use of this toolkit is for facilitating comparison of several different fMRI analysis methods.

Currently in the literature, several fMRI analysis methods are proposed. Unfortunately, the performance of most of these methods are shown on real fMRI data, which embodies a myriad of unrepeatable artifacts, specific to the session, subject and task within which the data is acquired. Although there are a few Internet sites from which actual fMRI data can be downloaded for comparing the performance of multiple fMRI analysis methods, these real fMRI datasets are not modifiable. Because the real data does not allow modification and incorporation of different noise levels, it is hard to investigate the performance boundaries of the proposed analysis methods. At which noise level are two methods equal? At which noise level a proposed method performs superior to other methods? These are important questions which cannot be answered currently, due to the lack of a gold-standard in fMRI data acquisition.

The simulated fMRI toolbox developed in this study serves as a dynamic testbed through which, all fMRI data analysis methods can be compared. The format of the data generated in our toolbox conforms to ANALYZE format, which is a widely accepted

data format in fMRI research. The fMRI data created in our toolbox allows for incorporating head motion, cardiac pulsation, scanner drift and habituation type noise artifacts. Although some of these artifacts (small head motion, cardiac pulse and scanner drift) can be processed and removed from the fMR time series before feeding into the fMRI analysis pipeline, some of these artifacts (large head motion, habituation) cannot be accounted during data pre-processing, and has disrupting effects in fMRI analysis. Therefore, our toolkit provides a strong means for investigating the success of fMRI analysis in the presence of this kind of disruptive noise.

In addition, our toolbox is capable of generating fMRI data based on experimental design parameters. Block, event related design parameters can be flexibly given by the user in order to create desired experimental designs.

Finally, our toolkit allows for generation of a series of full brain fMRI data. The importance of this lies in the fact that, recently, in fMRI analysis, there is a trend to perform data analysis with spatio-temporal approaches. Furthermore there are new methods such as Dynamical Casual Model through which multiple loci of activations are investigated. Our toolkit also allows generation of multiple activity loci which is an important attribute. To the best of our knowledge the fMRI toolkit presented here is the first simulator which embodies a whole brain time series. This will allow for researchers to study spatial performance of their fMRI analysis techniques.

In the future, other noise sources like respiratory activities could be added. Most importantly, cognitive noise could be added. Our toolkit was planned to be distributed as an open source software from [brain.ii.metu.edu.tr](http://brain.ii.metu.edu.tr). Therefore, the methods used in this study can be disseminated to the whole neuroimaging community in the future.

## REFERENCES

- Baghdadi, L. (2004, May 26). *Introduction to MINC 2.0*.  
[http://www.bic.mni.mcgill.ca/software/minc/05-2004MINC20-tutorial\\_lb.pdf](http://www.bic.mni.mcgill.ca/software/minc/05-2004MINC20-tutorial_lb.pdf)
- Benoit-Cattin, H., Collewet, G., Belaroussi, B., Saint-Jalmes, H., & Odet, C. (2004). The SIMRI project : A versatile and interactive MRI simulator. *Journal of Magnetic Resonance* , 30.
- Buxton, R. B., & Frank, L. R. (1997). A Model for the Coupling Between Cerebral Blood Flow and Oxygen Metabolism During Neural Stimulation. *Journal of Cerebral Blood Flow and Metabolism* , 64-72.
- Buxton, R. B., Wong, E. C., & Frank, L. R. (1998). Dynamics of Blood Flow and Oxygenation Changes During Brain Activation: The Balloon Model. *Magnetic Resonance in Medicine* , 855-864.
- Cocosco, C. A., Kollokian, V., Kwan, R.-S., & Evans, A. C. (1997). BrainWeb: Online Interface to a 3D MRI Simulated Brain Database. *NeuroImage* .
- Drobnjak, I., Gavaghan, D., Süli, E., Pitt-Francis, J., & Jenkinson, M. (2006).

Development of an fMRI Simulator for Modelling Realistic Rigid-Body Motion Artifacts. *Magnetic Resonance in Medicine* .

Friston, K. J., Mechelli, A., Turner, R., & Price, C. J. (2000). Nonlinear Responses in fMRI: The Balloon Model, Volterra Kernels, and Other Hemodynamics. *NeuroImage* , 466-477.

Holodny, A. I. (2008). *Functional Neuroimaging: A Clinical Approach*. Informa.

Huettel, S., Song, A. W., & McCarthy, G. (2004). *Functional Magnetic Resonance Imaging*. Sinauer.

Jochimsen, T. H., & Mengershausen, M. v. (2004). *ODIN—Object-oriented development interface for NMR*. Germany.

Rew, R., Davis, G., Emmerson, S., & Davies, H. (1997). *NetCDF User's Guide for C, An Access Interface for Self-Describing, Portable Data*. Boulder: Unidata Program Center.

Sled, J. G., Vincent, R. D., & Baghdadi, L. (2004, May 28). *MINC 2.0 User's Guide*. [http://www.bic.mni.mcgill.ca/software/minc/minc2\\_uguide/](http://www.bic.mni.mcgill.ca/software/minc/minc2_uguide/)

Smith, S. M., Jenkinson, M., Woolrich, M. W., Beckmann, C. F., Behrens, T. E., Johansen-Berg, H., et al. (2004). Advances in functional and structural MR image analysis and implementation as FSL. *NeuroImage* , 208-219.

Vahedipour, K., Shah, N. J., & Stöcker, T. (2008). Jemris 2.0: High Performance Computing Simulator for MRI. *26th ESMRMB*. Valencia.

Vincent, B., Baghdadi, L., & Sled, J. G. (2004, Feb 01). *MINC 2.0 Application Programming Interface (API)*. [http://www.bic.mni.mcgill.ca/software/minc/minc\\_20/](http://www.bic.mni.mcgill.ca/software/minc/minc_20/)

Vincent, R. D. (2005, May 10). *The MINC 2.0 File Format*. [http://www.bic.mni.mcgill.ca/software/minc/minc2\\_format/](http://www.bic.mni.mcgill.ca/software/minc/minc2_format/)

# APPENDIX

## A. Anatomical Directions and Planes

